LABPLAS

Horizon 2020
European Union Funding
for Research & Innovation

Land-Based Solutions for Plastics in the Sea

This project has received funding from the European Union's Horizon 2020 research and innovation programme under grant agreement No 101003954

D3.5 Report on methodological guidelines, and quality control and assurance approaches to identify MP in field samples

Due date of deliverable: 31/03/2025

Actual submission date: 31/03/2025

Horizon 2020
European Union Funding
for Research & Innovation

LABPLAS

Horizon 2020
European Union Funding
for Research & Innovation

PROJECT INFORMATION

Project number: 101003954

Project acronym: LABPLAS

Project full title: Land-Based Solutions for Plastics in the Sea

Call: H2020-SC5-2018-2019-2020 submitted for H2020-SC5-2020-2 / 03 Sep 2020

Topic: CE-SC5-30-2020 – Plastics in the environment: understanding the sources, transport, distribution and impacts of plastics pollution

Type of action: RIA – Research and Innovation Action

Starting date: June 1st, 2021

Duration: 48 months

List of participants:

Nº	Participant name	Acronym	Country	Type
1	UNIVERSIDADE DE VIGO	UVI	SPAIN	HES
2	UNIVERSIDADE DA CORUÑA	UDC	SPAIN	HES
3	Bundesanstalt fuer Gewaesserkunde	BfG	GERMANY	RTO
4	LABORATORIO IBERICO INTERNACIONAL DE NANOTECNOLOGIA	INL	PORTUGAL	RTO
5	KATHOLIEKE UNIVERSITEIT LEUVEN	KUL	BELGIUM	HES
6	HELMHOLTZ ZENTRUM FUR OZEANFORSCHUNG KIEL	GEOMAR	GERMANY	RTO
7	NATIONAL OCEANOGRAPHY CENTRE	NOC	UNITED KINGDOM	RTO
8	SORBONNE UNIVERSITE	SU	FRANCE	HES
9	OPEN UNIVERSITEIT NEDERLAND	OUNL	NETHERLANDS	HES
10	LEIBNIZ INSTITUTE FOR BALTIC SEA RESEARCH	IOW	GERMANY	RTO
11	ASSOCIACAO PARA O DESENVOLVIMENTO DO ATLANTIC INTERNATIONAL RESEARCH CENTRE	AC	PORTUGAL	RTO
12	UNIVERSIDADE FEDERAL DO SAO PAULO	UNIFESP	BRAZIL	HES
13	BASF SE	BASF	GERMANY	LE
14	TG ENVIRONMENTAL RESEARCH	ER	UNITED KINGDOM	SME
15	CONTACTICA S.L.	CTA	SPAIN	SME
16	STICHTING EGI	EGI	NETHERLANDS	Non-P
17	STICHTING RADBOUD UNIVERSITEIT	RU	NETHERLANDS	HES
18	UNIVERSIDADE FEDERAL DO PARÁ	UFPA	BRAZIL	HES

DELIVERABLE DETAILS

Document Number:	D3.5
Document Title:	Report on methodological guidelines, and quality control and assurance approaches to identify MP in field samples
Dissemination level	PU – Public
Period:	RP3
WP:	WP3
Task:	Task 3.5
Status:	Final
Coordinator	S. Muniategui-Lorenzo UNIVERSIDADE DA CORUÑA
Authors:	S. Muniategui Lorenzo; M.E del Castillo-Busto; A. López Rosales; V. Fernández-González; C. Moscoso-Pérez; J.M. Andrade; J. Ivar do Sul; R. Rodríguez; M.L. Pedrotti; K. Pabortsava; F. Stock. UNIVERSIDADE DA CORUÑA bfg HOW GEOMAR SORBONNE UNIVERSITÉ
Recommended citation format	S. Muniategui Lorenzo; M.E del Castillo-Busto; A. López Rosales; V. Fernández-González; C. Moscoso-Pérez; J.M. Andrade; J. Ivar do Sul; R. Rodríguez; M.L. Pedrotti; K. Pabortsava; F. Stock. 2025. Methodological guidelines, quality control and assurance approaches to identify MP in field samples, Deliverable 3.5, LABPLAS Grant Agreement No. 101003954 H2020-SC5-2020-2
Abstract:	This report corresponds to Deliverable 3.5, Report on methodological guidelines, and quality control and assurance approaches to identify MP in field samples resulting from Task 3.5 of the LABPLAS project. It also summarizes the results of the second-year sampling campaigns from WP2, covering various environmental matrices: surface microlayer water and small microplastics (10 µm–1 mm) from the Elbe, Thames, and Mero-Barcés rivers; bulk river sediments and core samples; MP ingestion by planktonic and benthic invertebrates; biota; and atmospheric deposition in the Elbe, Thames, and Mero-Barcés case studies. The report discusses the characterization of MP emissions from road dust and water runoff in the Mero-Barcés case study (WP3 Task 3.3.2). This includes analysis of road dust and water runoff samples, the assessments conducted using the block platform for urban drainage and runoff studies, and wastewater analysis. Drawing on the experience gained in the LABPLAS project, the report provides recommendations and guidelines (WP3 Task 3.5) for

	evaluating the effectiveness and limitations of different MP detection techniques. These considerations include measurable particle size ranges, mass determination, best practices for MP extraction and purification, and comprehensive quality assurance (QA) and quality control (QC) measures. Specific guidelines are provided for contamination control, blank tests, and ensuring high-quality analytical results.

Version	Date	Comments
1.0	29/11/2024	First version - Proposed methodological guidelines, and quality control and assurance approaches to identify MP in field samples
2.0	31/03/2025	Second version – Final

Disclaimer

The views and opinions expressed in this document reflect only the authors' views, and not necessarily those of the European Commission.

TABLE OF CONTENTS

LIST OF FIGURES

LIST OF TABLES

ABBREVIATIONS AND ACRONYMS

Abbreviation / Acronym	Description
ABS	Acrylonitrile-butadiene-styrene
EGB	East Gotland Basin
EVA	Ethylene-vinyl acetate
FPA	Focal plane array
FTIR	Fourier Transformed Infrared Spectroscopy
HQI	Hit quality index
QCL-LDIR (or LDIR)	Quantum-cascade Laser-based transflectance Infrared spectroscopy
MCA	Medieval Climate Anomaly
MPs	Microplastics
6PPD	N-Phenyl-N'-(1,3-dimethylbutyl)-p-phenylenediamine
PA	Polyamide
PAHs	Polycyclic aromatic hydrocarbons
PC	Polycarbonate
PE	Polyethylene
PE-Cl	Polyethylene-Cl
PET	Polyethylene terephthalate
PLA	Polylactic acid
PMMA	Polymethyl methacrylate
POM	Polyoxymethylene
PP	Polypropylene
PS	Polystyrene
PTFE	Polytetrafluoroethylene
PU	Polyurethane
PVC	Polyvinyl chloride
Py-GC-MS	Pyrolysis- gas chromatography- mass spectrometry
QA	Quality assurance
QC	Quality control
QCL	Quantum-cascade laser-based imaging system
RDS	Road dust samples
SBR	Styrene-butadiene rubber
SML	Surface microlayer
SPE	Solid-phase extraction
TMQ	2,4-Trimethyl-1,2-dihydroquinoline
TOC	Total organic carbon
TSS	Total suspended solids
WWTP	Waste-water treatment plant
XRF	X-ray fluorescence

1 INTRODUCTION

This document constitutes Deliverable D3.5, which provides a comprehensive report on the methodological guidelines and quality control (QC) and quality assurance (QA) approaches for identifying microplastics (MPs) in field samples, as outlined in Task 3.5.

It presents the results from samples collected during the second-year sampling campaigns in the North Sea, Thames River, Elbe River, and Mero-Barcés River Basin, covering multiple environmental compartments: water, sediment, air, and biota. It also incorporates description and results from the analysis of sediment core samples retrieved from the Gulf of Finland and the East Gotland Basin (EGB) in the Baltic Sea. These results were not included in Deliverable D2.4 of WP2 due to delays in these sampling campaigns.

Additionally, this document includes results and discussion from Task 3.3 on the characterization of MP emissions from road dust and water run-off in the Mero-Barcés case study (further details in Deliverable D3.3).

A comparison and evaluation of the methodologies for detecting MPs in water, sediment, biota, and air are also provided. For each technique, general limits (e.g., particle size, mass, and polymer type) are specified, with a particular focus on defining the minimum measurable particle size (in µm). The recommended best practices for MPs extraction and purification are presented, emphasizing polymer preservation and effective matrix removal.

2 RESULTS OF SECOND-YEAR SAMPLING CAMPAIGNS

2.1 Surface microlayer

The sample treatment and the results for surface microlayer (SML) samples from the North Sea (Summer/Winter 2023) and the Elbe sampling campaign (2023) have been completed and presented in D2.4. The findings have been analysed, and a publication is currently in preparation.

2.2 Small microplastics (10 µm–1 mm) pump filtration

2.2.1 Small microplastics (10 µm–1 mm) – sample and data status

All the samples from the Thames, the Elbe, the North Sea, and the Mero Barcés (Spain) have been processed (i.e. MPs extracted) and analysed for the presence of small MPs using Fourier Transform Infrared Spectroscopy (FTIR) imaging technique at 25 µm resolution. The data on abundance (by count and mass) and morphological characteristics (e.g. particle area, size, etc) of MPs are now available for all the Thames, Elbe, and North Sea samples. The concentrations and characteristics of MPs in the samples collected in 2022 in the Elbe, Thames, and the North Sea were reported in Deliverable D2.4. The updated datasets from seasonal sampling in two rivers in 2023 are shown in Figure 1 - Figure 5. Data on MPs abundance by number and mass in the Mero-Barcés are given in Figure 6 and Figure 7. These data require blank correction (all the field/procedural blanks were processed and IR-imaged). The IR data also require additional examination to identify, quantify and characterise large particles present in the samples but not picked up by SiMPLe software.

2.2.2 Small microplastics (10 µm–1 mm) in the Elbe and the Thames – seasonal sampling in 2023

The abundance (by particle number and mass) and polymer diversity of MPs varied during 2023 in both rivers (Figures 1-4). The number concentrations of MPs were on average higher and more variable in the urban Dessau (6098 ± 6984 MPs m^{-3}) compared to the estuarine Cuxhaven (727 ± 387 MPs m^{-3}). Similarly, the number concentrations of MPs in the urban Victoria Docks (1693 ±1269 MPs m^{-3}) exceeded those in the estuarine Chapman Buoy (420 ± 371 MPs m^{-3}) (Figure 1). Remarkably high number concentrations of MPs

(16150 particles m^{-3}) were measured at the Dessau site in April 2023 and exceeded the concentrations of MPs measured in both Elbe and Thames in all other months (Figure 1A).

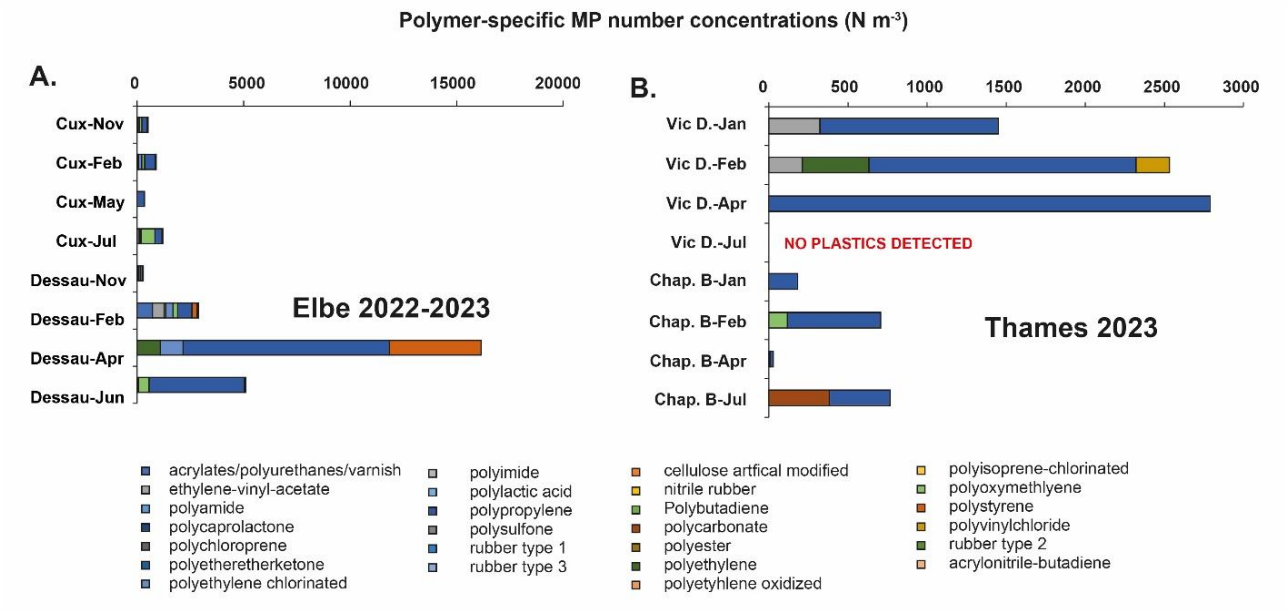

Figure 1: Polymer-specific microplastic number concentrations in the filtered water samples collected in the Elbe (A) and the Thames (B) in different seasons of 2023.

Mass concentrations of MPs followed a similar pattern in both rivers (Figure 2), with higher average loads of MPs measured in the urban site of the Elbe (10770 ± 9449 MPs m^{-3}) and the Thames (624 ± 633 MPs m^{-3}), compared to estuarine locations (5710 ± 9597 µg MPs m^{-3} and 82 ± 42 µg MPs m^{-3}, respectively). Overall, the Elbe sites were significantly more polluted with MPs compared to the Thames (8240 ± 9222 µg MPs m^{-3} and 353 ± 523 µg MPs m^{-3}, respectively).

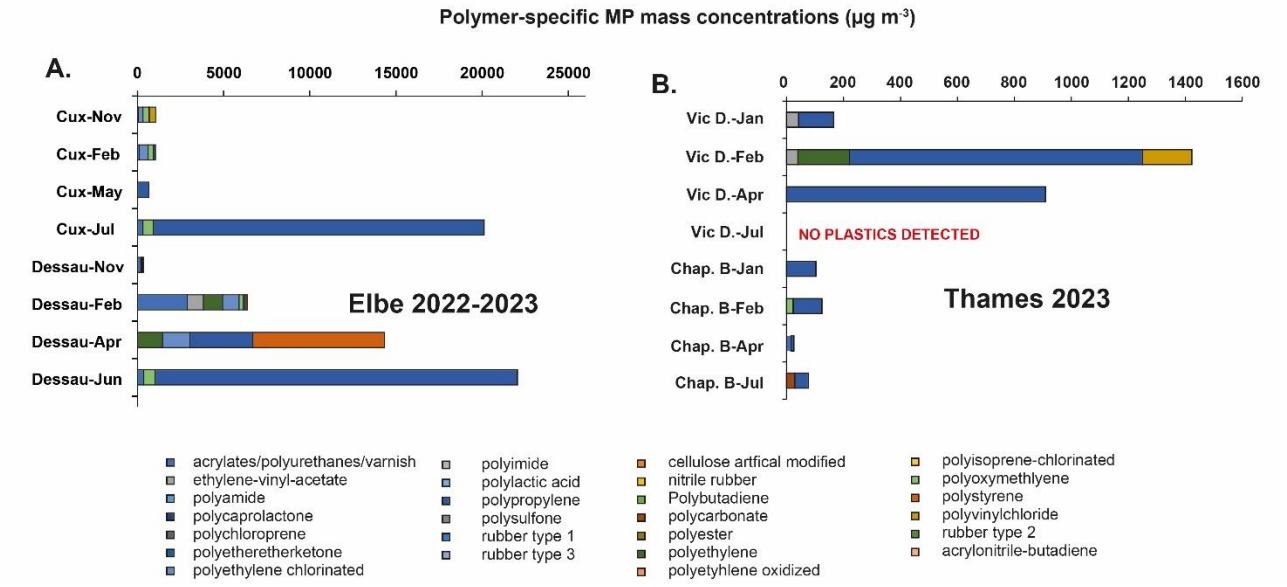

Figure 2: Polymer-specific microplastic mass concentrations in the filtered water samples collected in the Elbe (A) and the Thames (B) in different seasons of 2023.

Polypropylene (PP) was the most common polymer at all locations in both the Elbe and the Thames, with percentage contribution spanning 48-83 % by number concentrations (Figure 3) and 56-87 % by mass (

Figure 4). There were differences in overall polymer composition between the sites in two rivers (Figure 3 and

Figure *4*). Polyoxymethylene (POM) had a substantial presence in the estuarine samples in both Elbe and Thames (Figure 3A, C and

Figure *4*A, C, respectively). The contribution of this polymer to MPs load in Elbe samples was significantly lower in 2023 (3-32 %) than that measured in 2022 (28-84 %, all by number concentrations). In the Thames, the overall contribution from Acrylates/Polyurethanes/Varnishes dropped significantly in the samples from 2023 compared to the 2022 data with these polymers being detected only at Chapman Buoy in April 2023 (Figure 3 C, D and

Figure *4*C, D).

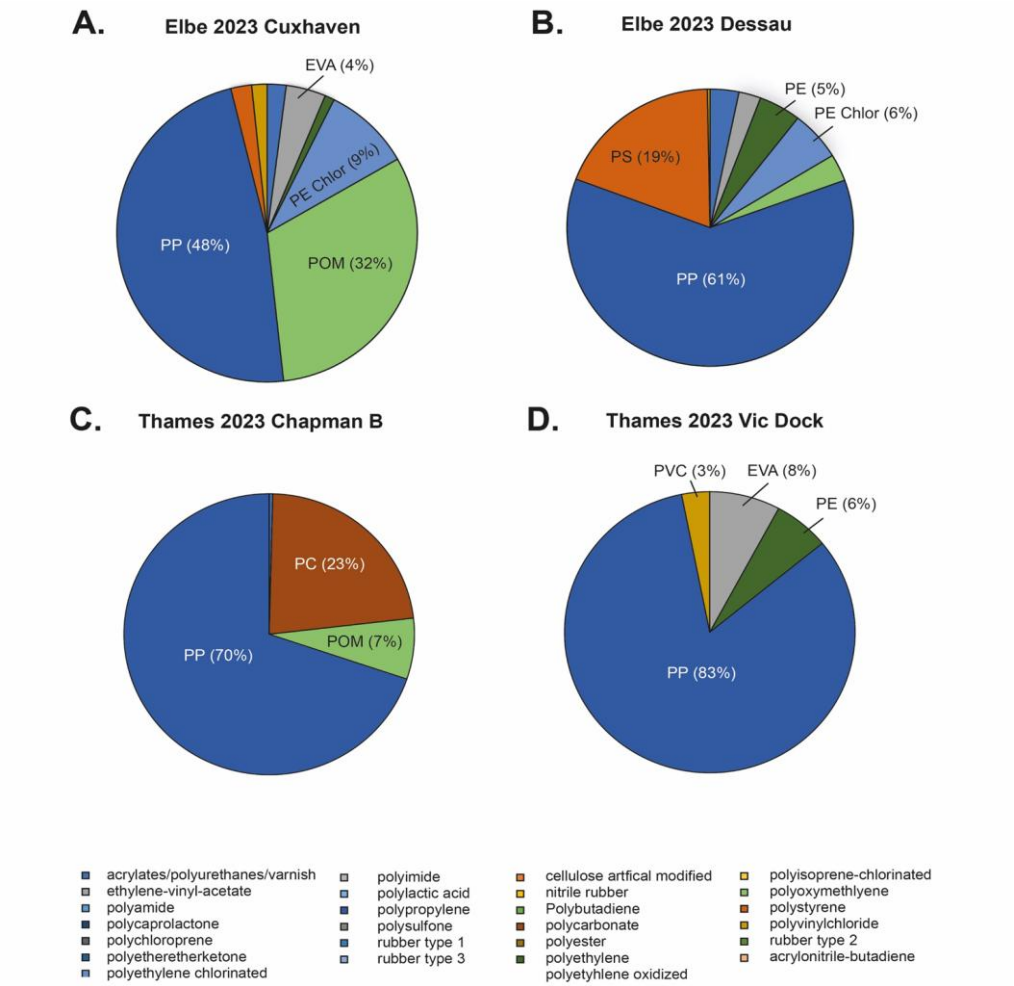

Figure 3: Polymer composition of microplastic particles (by polymer count) detected in the filtered samples from the Elbe (A, B) and the Thames (C, D) collected in different months of 2023.

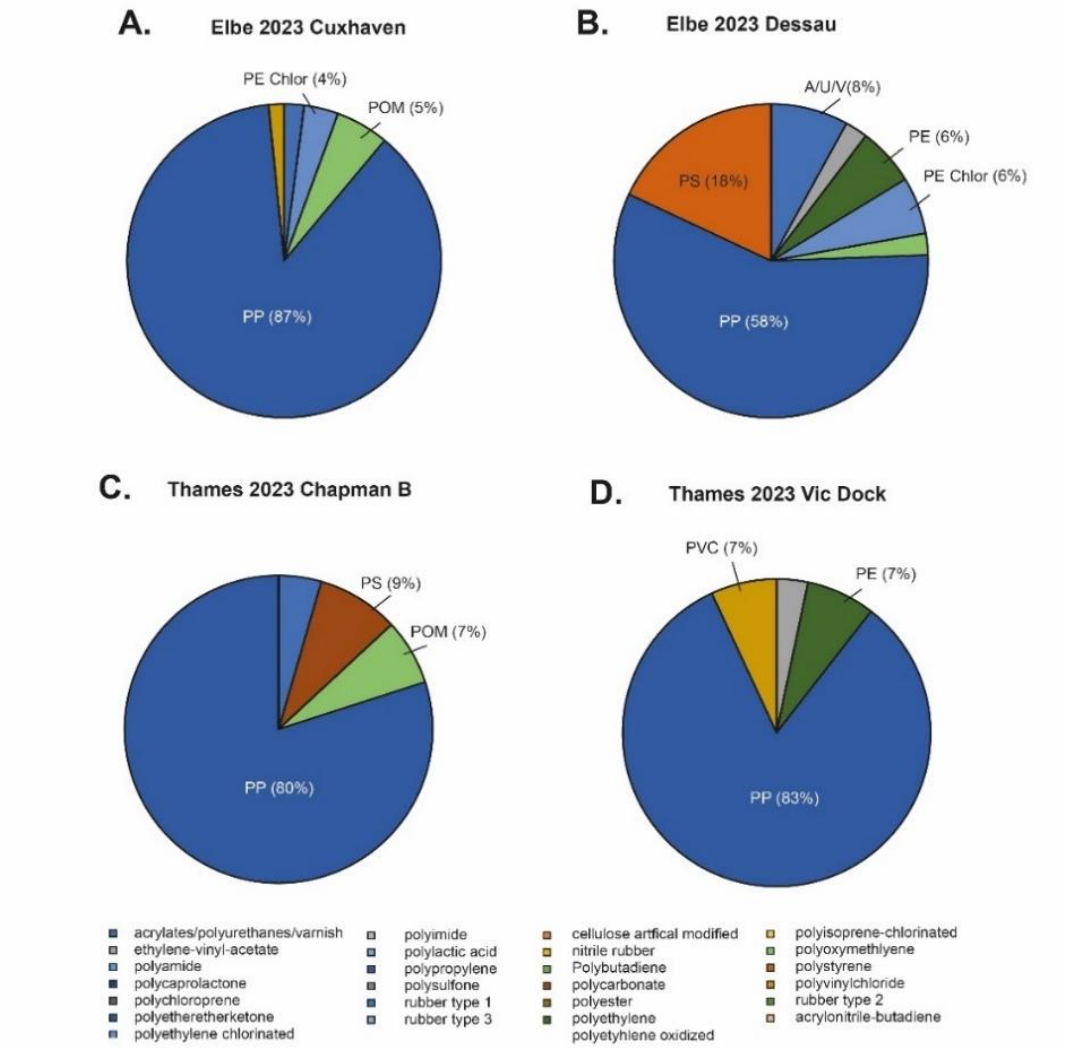

Figure 4: Polymer composition of microplastic particles (by polymer mass) detected in the filtered samples from the Elbe (A, B) and the Thames (C, D) collected in different months of 2023.

Microplastics with sizes < 100 μm dominated in both rivers (as Feret diameter; Figure 5). Microplastics were on average smaller in the Thames sites (93 ± 50 μm) than in the Elbe (120 ± 208 μm), consistent with 2022 measurements.

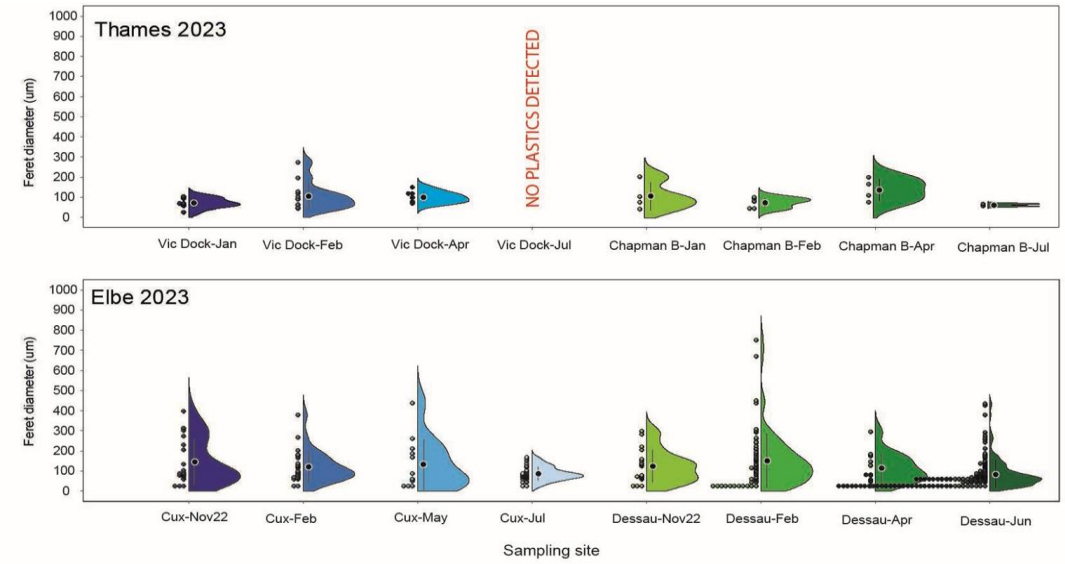

Figure 5: Particle size distribution data (as Feret diameter) for seasonal samples from the Thames (A) and Elbe (B) collected in different months of 2023. Data points making up the distributions are shown as circles of the respective colour. The width of each distribution was scaled to be equal to allow the inter-comparison of the distributions regardless of the number of data points. The black circles indicate mean particle sizes with horizontal bars as ± standard deviation.

2.2.3 Small microplastics (10 μm–1 mm) in the Mero-Barcés (Spain)

Polymer-specific MPs abundance by particle number and mass in Mero-Barcés are given inFigure 6 and Figure 7, respectively. The number concentrations and polymer composition of MPs in the Mero-Barcés varied among the sites and sampling period (Figure 6 A-C). The highest concentrations of MPs were measured at the Guiliade site in the summer of 2022 (1538 MPs m^{-3}) and winter of 2023 (3714 MPs m^{-3}), and at Cecebre beach in the summer of 2023 (23499 MPs m^{-3}). The least polluted site was Cecebre Bridge 2 in the summer of 2022 (197 MPs m^{3}) and summer of 2023 (177 MPs m^{-3}), and the Meirama site (279 MPs m^{-3}) in winter 2023. Overall, the total number concentration of MPs increased from summer 2022 (680 ± 554 MPs m^{-3}) to winter 2023 (1321 ± 1237 MPs m^{-3}) and summer 2023 (5979 ± 8732 MPs m^{-3}). The seasonal sampling at two hotspot sites revealed higher mean concentrations at the Telva site (4922 ± 4503 MPs m^{-3}) compared to Guiliade (1265 ± 1379 MPs m^{-3}; Figure 6D).

By mass, the concentrations of MPs were consistently lowest at the Cecebre Bridge 2 site (Figure 7A-C). The elevated concentrations of MPs were observed at the Guiliade site in the summer of 2022 and winter and 2023. Exceptionally high concentrations of MPs were measured at Cecebre beach (247233 μg MPs m^{-3}) and Telva (600951 μg MPs m^{-3}) sites in the summer of 2023. Here, polyethylene (PE) dominated the MP load by mass at Cecebre beach, while artificially modified cellulose and polylactic acid (PLA) were dominant at the Telva site (Figure 7C).

At two hotspots sites, mean mass concentrations were higher at the Telva site (52817 ± 88859 μg MPs m^{-3}) compared to Guiliade (1861 ± 3158 μg MPs m^{-3}; Figure 7D) with remarkably high concentrations of 155408 μg MPs m^{-3} measured at Telva in July 2023 and dominated by Acrylates/Polyurethanes/Varnishes (Figure 7D).

PE and Acrylates/Polyurethanes/Varnishes were dominant at most of the sampling sites in the Mero-Barcés.

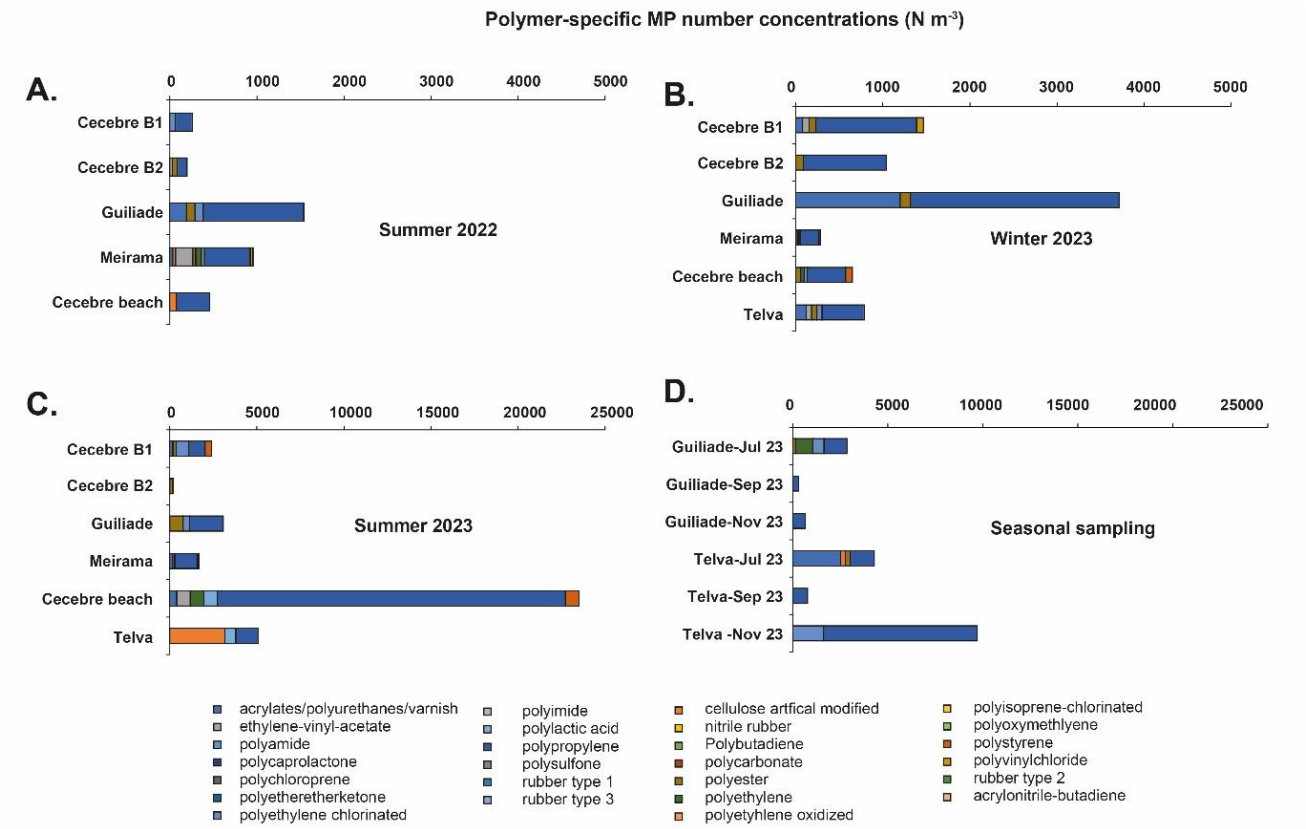

Figure 6: Polymer-specific microplastic number concentrations in the filtered water samples collected in the Mero Barces (Spain) in 2022 and 2023. (A) Summer 2022; (B) Winter 2023; (C) Summer 2023; (D) Seasonal sampling in 2023. These data are preliminary and require blank correction.

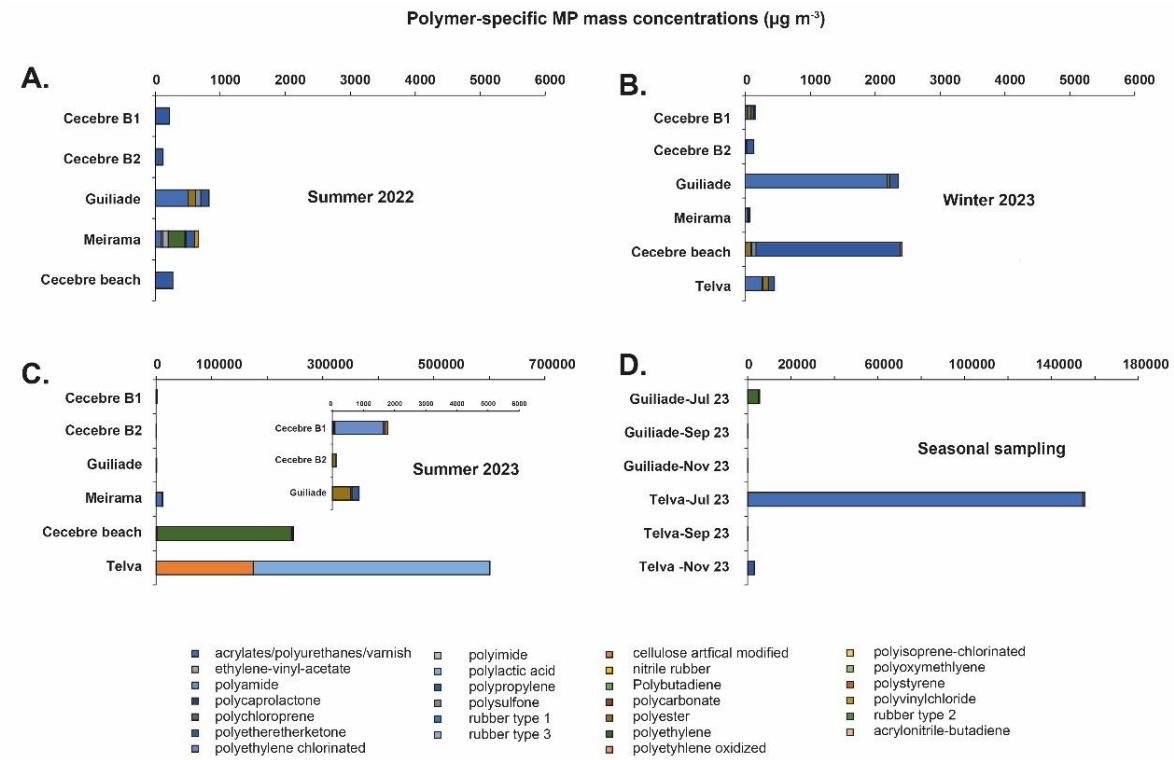

Figure 7: Polymer-specific microplastic mass concentrations in the filtered water samples collected in the Mero Barces (Spain) in 2022 and 2023. (A) Summer 2022; (B) Winter 2023; (C) Summer 2023; (D) Seasonal sampling in 2023. These data are preliminary and require blank correction.

2.3 Sediments

2.3.1 Bulk river sediment samples

Due to unforeseen circumstances, including the departure of the person previously responsible at BfG, only sediment samples from the first two sampling campaigns from Mero-Barcés were digested and analysed using LDIR at BfG. Subsequently, UDC has committed to conducting the treatment and analysis of the remaining seasonal campaign samples using LDIR in their laboratories in Spain. Different extraction protocols for MPs in sediments are being tested at UDC using salts of different densities, such as the potassium formate salt (density of ~ 1.58 g/cm^3) used by BfG. Results will be discussed in a dedicated scientific publication.

The MP extracted from approximately 50 g (if available) of each size fraction (10-100 µm and 100-1000 µm) was measured on a separate Kevley (low-e IR reflective) slide. The results were combined to present data for the entire sample (for more details, see progress report of WP2, 2022). As with other samples from the Thames River, Elbe River and North Sea, measuring the smaller size fraction (10-100 µm) involved analysing up to 20,000 particles, making the process highly time-consumptive (up to two weeks per sample). The measured spectra were compared to a reference in-house library. For the Mero-Barcés, all spectra with a match of > 0.90 (rubber > 0.95) were used for the analysis. Procedural blanks were prepared in the laboratory of the German Federal Institue of Hydrology. As with other analysis, the blanks were processed in the same way as MP sediment samples (see SOP, D2.2). The blank contained 4 PA and 1 POM. None of the samples have been corrected for blank value.

The total numbers of MPs per kg for the Mero-Barcés samples are shown in Figure 8, with the MP size distribution presented in Figure 9 and polymer-specific MP data per sampling site in Figure 10.

The total concentration of MPs varied between seasons and among sampling sites. Winter samples (sampling 2) revealed higher concentrations than spring samples (sampling 3) (mean ± std in winter: 573 ± 478 MPs/kg and 277 ± 266 MPs/kg in spring; winter min. 58 MPs/kg, max. 1204 MPs/kg; spring min. 16 MPs/kg, max. 676 MPs/kg). In winter, the samples MB1 and MB2 have more than 800 MPs/kg and MB6 and MB7 <200 MPs/kg. In spring, the highest number of MPs was detected in MB6 (676 MPs/kg), followed by MB1. MB2, which had the highest values in winter, showed almost no MPs in spring.

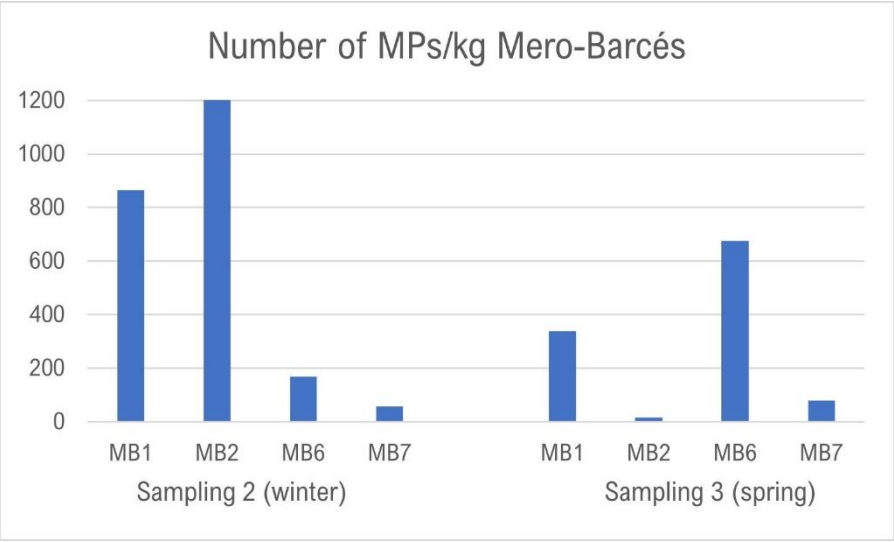

Figure 8: Number of MPs in the Mero-Barcés River Basin (samplings 2 (winter) and 3 (spring))

For the different size classes (Figure 9), only half of the samples have more than 50 % of MPs in the smallest size class (10-100 µm). Only sample MB6 has MPs in the largest size range (300-1000 µm).

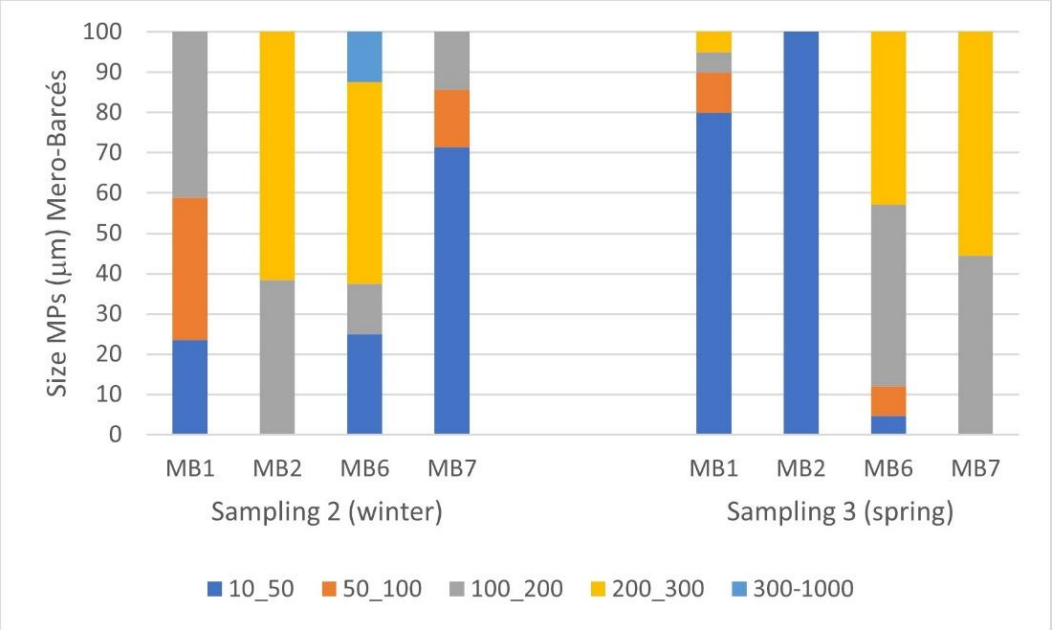

Figure 9: Size fraction of the MPs from Mero-Barcés River Basin (samplings 2 (winter) and 3 (spring))

The polymer composition of MPs varied between sites and seasons. The most common polymers were PP, PE, PA and the unified class Acrylates/PU/Varnish. In winter, PP dominated the samples, whereas in spring, its proportion was much smaller. PET and PTFE were present in spring but absent in winter. In sample MB2 during spring, only acrylonitrile butadiene was found.

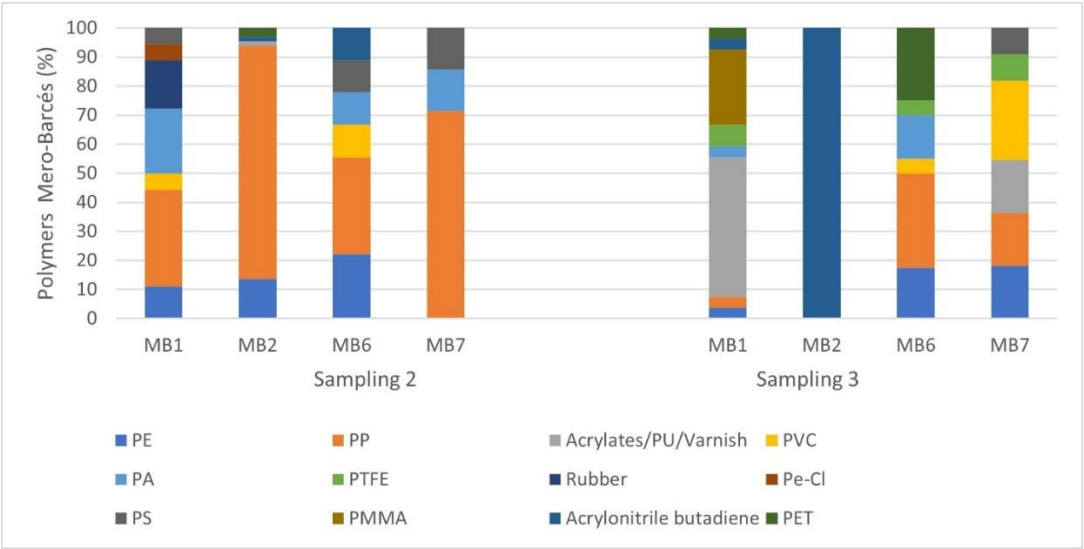

Figure 10: Polymer composition of MPs in the Mero-Barcés River Basin (samplings 2 (winter) and 3 (spring)).

2.3.2 Sediment core samples

This study is focused on the analysis of MPs in sediment cores from the Baltic Sea, trying to determine whether there is a distinct transition in MP concentrations and polymer composition between the Holocene and the Anthropocene. According to the Anthropocene Working Group, the Anthropocene began in 1952 and can be extensively recognised by the occurrence of artificial radionuclides and other anthropogenic markers, including MPs, in sediment archives worldwide (Waters et al., 2024). Here results from samples from the Gulf of Finland sediment core are presented.

Core location and sampling

The core was taken from the Baltic Sea, a shallow marginal sea with an average depth of 55 m, characterised by estuarine circulation. The upper water layer has low salinity due to high freshwater input from rivers in the eastern and northern parts of the catchment. This dense water from the North Sea spreads into deep layers and causes a strong vertical salinity gradient in the central Baltic Sea, with a pronounced halocline at about 60-80 m depth. Approximately 85 million people live in the Baltic Sea catchment area. In the southern part of the Baltic Sea, 65 % of the land area is used for agriculture (Kaiser et al., 2023).

One sediment core was retrieved from the Gulf of Finland (GOF EMB262/12-2 MUC 3) (59°34.443'N, 023°36.461'E, Water Depth: 81) during the expedition EMB262 "PHYTOARCHIVE" on board the research vessel Elisabeth Mann Borgese. A multi-core, equipped with 60 cm-long PVC tubes, was used to ensure the water-sediment interface remained undisturbed. The core was then opened lengthwise on board and stored in the core repository of the IOW at a low temperature.

Sampling and extraction of MPs from sediments

Potential MPs (particle size between 20 µm and 5 mm) were extracted and isolated from sediments at IOW (Germany), following a well-established protocol (Enders et al., 2020). After freeze drying, the sediments were first submitted to density separation using sodium polytungstate (1800 kg m^{-3}) to reduce the inorganic matter content of a sample. Density separation was performed in separation funnels. The flask was shaken a few times before the solution was left to settle to guarantee the separation liquid was in contact with all particles in the sample. The remaining material was then digested with 30 % H_2O_2 to eliminate the organic content of the sample. The recovery rate of the method was estimated to be 80 % and both fibres and fragments were successfully extracted.

Analysis of MPs' identity using LDIR

All suspect particles on the filter were analysed and counted using the Agilent 8700 LDIR analyser (Agilent Technologies), following the instructions in the instrument manual. The LDIR analyser uses a quantum cascade laser (QCL) as a light source and is equipped with fast scanning optics for efficient wavelength scanning. The LDIR analysis was used in the particle analysis mode and MP spectral library construction for automatic detection (Hildebrant et al., 2020, Hildebrandt et al., 2022). The system used image analysis techniques to determine the boundary and dimensions of the particle. In addition, a full spectrum of each particle, covering the range of the instrument, was collected and compared to the spectral library in real-time. The spectra obtained were compared to the library provided by Agilent Technologies (Microplastic Starter 1.0). This library was extended with a variety of spectra of plastic polymers and natural components (Hildebrandt et al., 2022). Based on comparison with the spectral database, a minimum hit quality index (HQI) of 0.80 was established as a qualitative standard for MPs (including blanks). However, it varied for specific polymer types such as rubber (confidence > 0.90), PA and polyethylene-Cl (PE-Cl) (confidence > 0.85). Particles initially classified as rubber

and PA were excluded after being manually checked for inconsistences. Acrylates/PU/varnish also showed to be not easily distinguished from natural particles, particularly chitin and cellulose and did not reach the quality criteria to be assumed as plastic particles. Within the other polymer types, particles with an HQI of 0.85 were automatically accepted, while particles with an HQI between 0.80 and 0.85 were manually checked for inconsistencies. This involved manually checking over 500 individual particles. The morphology of MP was classified into two types: fibres with an aspect ratio of > 3 or < 0.33 (e.g., Whiting et al., 2022) and fragments. All samples were analysed at the Federal Institute of Hydrology in Koblenz.

The Gravity core as a baseline of contamination in the lab and field

Sediment core EMB262/6-30GC (57°17.022', 020°07.285'; 241m depth) was retrieved from the East Gotland Basin (EGB) during the expedition EMB262 "PHYTOARCHIVE" on board the research vessel Elisabeth Mann Borgese. In the laboratory, sediment layers between 94 and 104 cm depth corresponded to the Medieval Climate Anomaly (MCA; 1,200-700 years BP). The MCA has environmental conditions similar to those of the other cores analysed in this project. These samples are used here as background or baseline contamination for the MP laboratory and fieldwork. It also minimises extraction bias (i.e. if blanks have a different particle composition compared to the target samples) in relation to environmental and blank samples. The sediment was subjected to the MP extraction cascade in the same way as all other conventional samples. Two samples were analysed and a total of 16 plastic particles belonging to 3 polymer types were found: polytetrafluoroethylene (PTFE), polypropylene (PP), and polyethylene (PE). Particles measured between 20 and 367 µm. All particles were classified as fragments. These particles were blank-corrected by a combination of morphology, size and polymer type and excluded from the final dataset. All particles from the sediment samples and the procedural blanks were classified into 4 size categories according to their width. These were 20-50 µm, 51-100 µm, 101-200 µm and > 200 µm (Hildebrandt et al., 2022).

Quality Assurance and Control Procedures

A strict protocol was followed to prevent contamination of laboratory equipment, reagents, water and air. This included the rigorous use of laminar flow benches for sample handling, filtration of all reagents and water (10 µm stainless steel filters), use of cleaned metal or glass laboratory ware, use of cotton lab coats with sleeves and particle-free nitrile gloves and the performances of method blanks. Samples were blank corrected by a combination of particle characteristics (morphology, size fraction and polymer type). No contamination from the core tube was observed.

Results of the sediment core samples

Microplastics were successfully extracted and analysed in all layers of the core and control samples. The procedural blanks contained 10 MPs and revealed a relatively high diversity of polymers including PP, PTFE, polycarbonates (PC), polyethene terephthalate (PET), and polyvinyl chloride (PVC). No particles in the form of fibres were found in the control (blank) samples. This is an indication that air contamination in the laboratory was negligible.

A total of 201 MP particles were recovered and positively identified from the 15 sediment layers. Microplastic sizes varied between 20 and 508 µm, with an average size of 67.7 (± 65.8) µm. The MP abundance ranged from 0.18 to 30.53 MP particles per gram sediment DW (Figure 11A, data older than 1930 CE not shown). The highest concentration was found in the 11.25 cm layer (correspondent to 1966 CE) and the lowest concentration was found in the deepest analysed layer at 25.25 cm depth (1864 CE). No significant correlation was found between the abundance of MPs and the sediment depth (Persons, r=-0.433, p=0.106). This suggests an unclear

pattern of MP accumulation in sediments over time. There was a lack of a clear correlation (Persons, r=-0.111, *p*=0.858) between MP abundance in the core and global plastic production rates (including fibres) (Figure 11A).

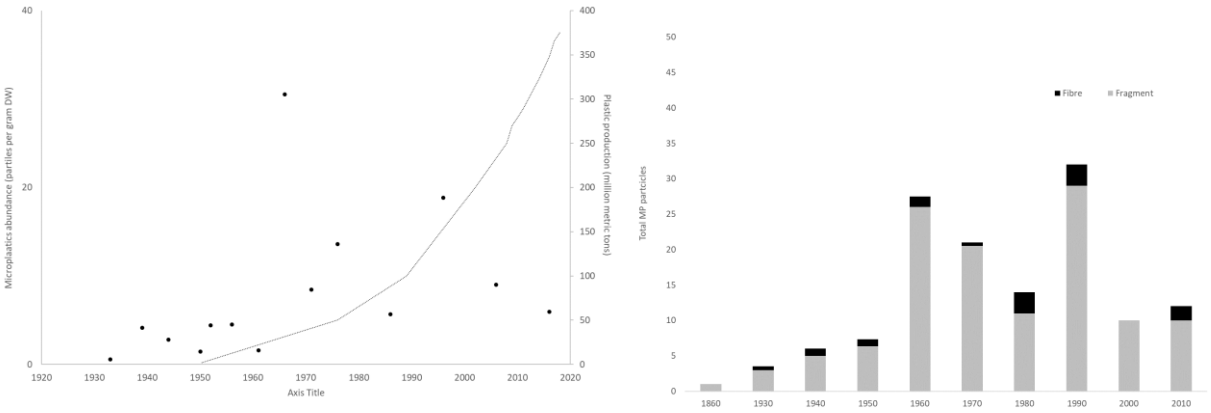

Figure 11: (A) Abundance of MPs extracted from the sediment core from 1933 to 2016 (left y-axis) and the annual global plastic production in million metric tons (right y-axis). (B) Total number of MPs classified as fibres and fragments from the 1860 decade and the 2010 decade. Where more than one data was available per decade, the number shown represents the average of the measures for fibres and fragments separately.

In general, there was a low contribution of fibres (N=17) compared to fragments (N=184) along the time series analysed in the Gulf of Finland (Figure 11B). Also, there is no consistent trend in the occurrence of fibres over time. In terms of polymer diversity, fibres were identified as belonging to 8 polymer types or clusters: PC, PE-Cl, PET, polymethyl methacrylate (PMMA), PP, PTFE, PS and PVC. Five of these (PC, PE-Cl, PET, PMMA, PS) were identified in one core layer only (one particle). On the other hand, PVC and PP fibres were relatively more frequent as they were identified in 3 core layers out of 10 core layers where any fibre was measured.

Fragments showed a relatively higher polymer diversity compared to fibres. Eleven polymer types or clusters were identified, including, PE, PLA (polylactic acid; one particle only) and polyoxymethylene (POM), in addition to all other polymer types identified as fibres (Figure 11B and Figure 12). The only polymer type that appears more frequently in all layers is PVC. This polymer cluster accounted for about 40 % of all the particles positively identified as plastics. There is no significant correlation (Persons, r= 0.42, p=0.112) between the total organic carbon (TOC %) in the sediment core layers and the abundance of MPs.

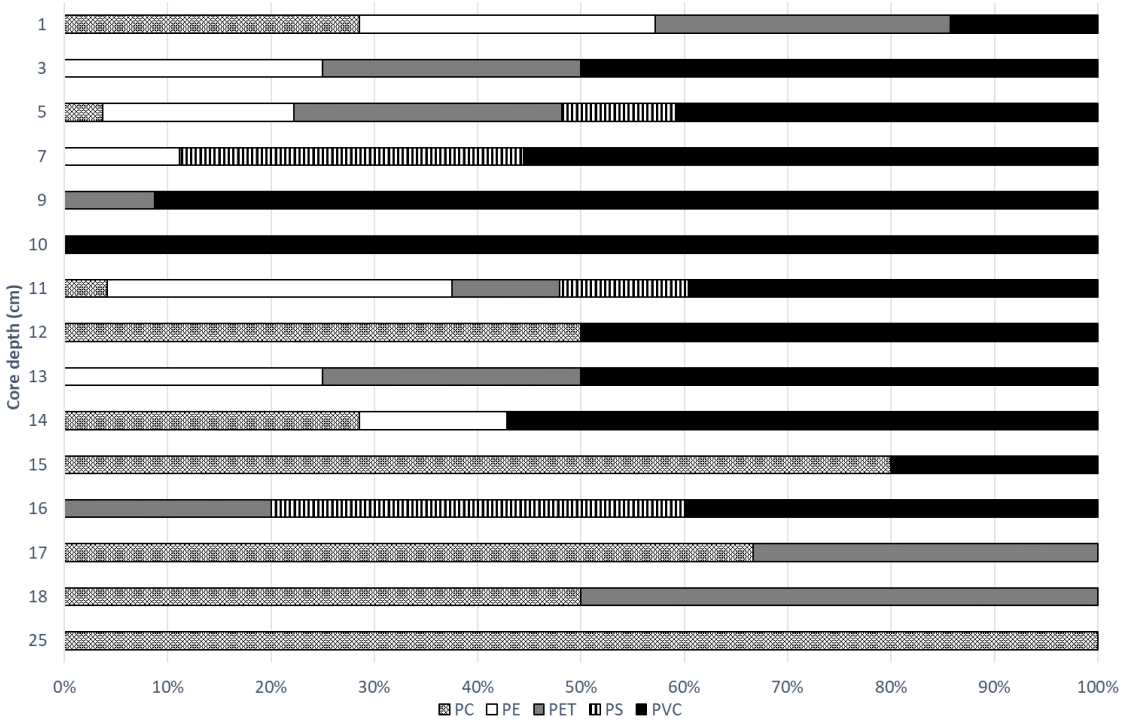

Figure 12: Microplastic polymer composition in the sediment profile. PE in the figure corresponds to PE and PE-Cl particles together. Polymers that are represented by less than 10 particles in all the core layers (PLA, POM, PMMA and PTFE) are not shown.

A very conservative approach was used here to finally attribute an identity to particles analysed in the sediment core layers. This is to avoid the overestimation of MPs in the core, as the MP particles here are ultimately used to define the Anthropocene Epoch in the Gulf of Finland sediment core. The next steps are to analyse and detail the composition and diversity of polymers in the East Gotland Basin sediment core, in an attempt to have a bigger picture of the MPs' temporal patterns in the Baltic Sea.

High priority has been given to analysing the core from the Gulf of Finland, followed by the East Gotland Basin (EGB) core, to integrate the data for publication. A draft of this paper is expected by May 2025. In parallel, a manuscript titled *"The Ultimate Guide of Microplastics in the Anthropocene"* is being prepared for submission to *Earth Science Reviews* by May 2025, and a perspective paper on MPs in the ocean has been resubmitted to *Environmental Research Letters*.

2.4 Ingestion of MPs by planktonic and benthic invertebrates

Concentrations of micro-, meso- and macroplastics in water together with the concentrations of different zooplankton organisms have been quantified and reported in the previous deliverable “D2.4 Sample preparation - Results of 2nd year and suggestions for sampling SMNPs”. The indicator plastic: zooplankton ratio has been also studied for each station and the information was reported in “Deliverable 3.4. Report on MP and zooplankton indicator from analysed field samples”.

Regarding the analysis of MP ingestion by planktonic and benthic invertebrates, the organisms of interest have been isolated from each sample, and enzymatic digestion has been performed in all the samples at SU. The resulting digested samples were subsequently analysed and each particle was characterized using LDIR at UDC. This deliverable presents ingestion data for planktonic invertebrates, specifically copepods, across the three study aquatic systems.

A total of 67 samples, representing a total of 11520 individual copepods, were analysed. The results show an average MPs ingestion rate of 0.20 ± 0.07 MPs ind.$^{-1}$ across the three aquatic systems. However, the ingestion rate varied among locations: the North Sea exhibited the highest average value of MPs ingestion (0.39 ± 0.18 MPs ind.$^{-1}$) followed by the Thames River (0.18 ± 0.10 MPs ind.$^{-1}$) and the Elbe River (0.05 ± 0.01 MPs ind.$^{-1}$). Samples have been grouped into three regions for each aquatic system. Therefore, each region included multiple sampling stations (Upstream_TR, Central_TR, Dowstream_TR, West_NS, Central_NS, East_NS, Downstream_ER, Central_ER and Upstream_ER). Spatial variations in ingestion rates were observed within these described regions (Figure 13). The highest value was found in the central North Sea (0.71 MPs ind.$^{-1}$), which is very close to the value observed in the Central Thames River with 0.61 MPs ind.$^{-1}$. The lowest ingestion rate was observed in Central Elbe River with 0.008 MPs ind.$^{-1}$. The remaining stations exhibit more comparable ingestion values among themselves.

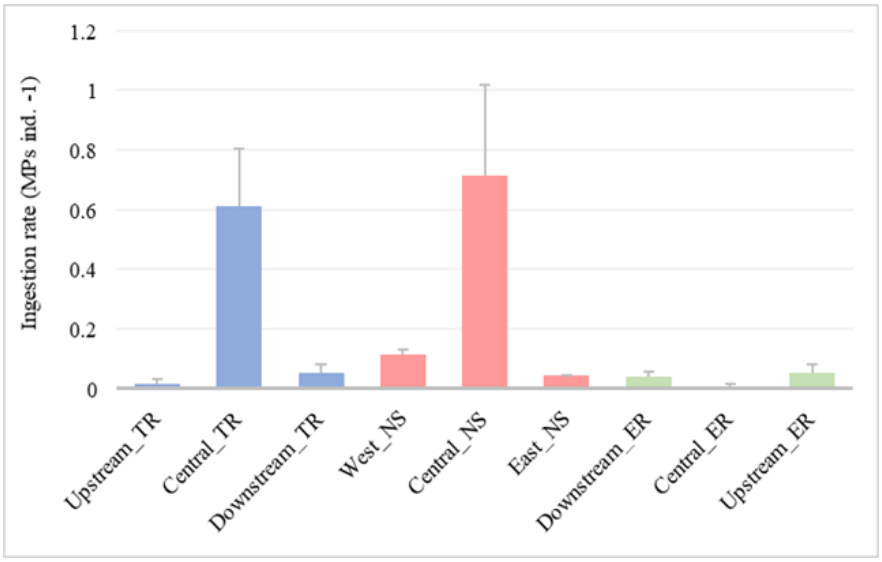

Figure 13: MPs ingestion rates (MPs ind^{-1}) in planktonic invertebrates (copepods) in Thames River (blue), the North Sea (red) and Elbe River (green). The locations are plotted in longitudinal order and each location groups several sampling stations. TR: Thames River, NS: North Sea and ER: Elbe River. Grey bars represent the standard error.

The high ingestion in the central Thames River may be attributed to its proximity to London, a densely populated urban area known for high plastic concentrations in the surrounding waters. In the case of the North Sea, the high ingestion could be explained by hydrodynamic processes that facilitate the regional accumulation of small plastic particles at the surface. To better understand the acquired ingestion rate results, we will integrate this information with the findings in other work packages, such as plastic concentration in water or modelled plastic distribution based on hydrodynamics.

Polymer identification has been performed in every sample with LDIR. This analysis displays a diverse range of ingested polymer types by planktonic invertebrates. Detected polymers include acrylate, ethylene-vinyl acetate (EVA), PET, PE, PMMA, PP, PS, PU, PVC, acrylonitrile butadiene styrene (ABS), rubber, alkyd varnish, PTFE, PA, and polyacetal. Another observation based on the particle's characterization performed is that the majority of ingested MPs belong to the smallest size range analysed (50-20 µm). This size range overlaps within the ingestion thresholds of the studied organisms.

PET is by far the most frequently ingested polymer in the three systems. In the Thames River, PET accounts for 71 % of the ingested polymers followed by 48 % in the North Sea and 22 % in the Elbe River. The second

most prevalent polymer is EVA, which is particularly highly ingested in the North Sea and Elbe River (27 % and 22 %, respectively). In contrast, PA is the second most ingested polymer in the Thames River (11 % of the polymer ingested in Thames are PA) (Figure 14).

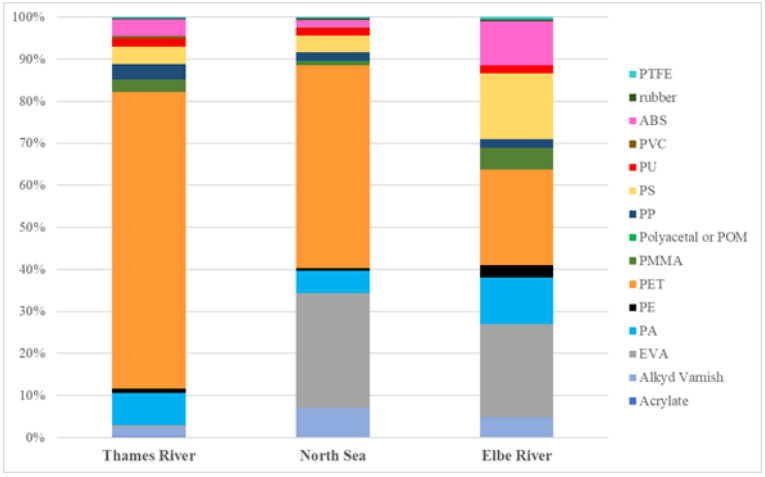

Figure 14: Percentage of polymer types ingested by copepods in the three aquatic systems: Thames River, North Sea and Elbe River.

We also have data on ingestion rates obtained using different sampling methods (manta or WP2) and across different seasons. These datasets will support further analyses, including the assessment of methodological and seasonal variations. In addition, all the collected data on ingestion rates and particle characterization will be integrated with information from other research groups within the project, focusing on MP distribution in aquatic systems. Combined with ecological data on copepods, this integrated approach will allow us to perform an accurate assessment of MP exposure risk and, consequently, ingestion by copepods in each region. A comprehensive analysis and interpretation of these results will be presented in a scientific manuscript that is under preparation for publication in a peer-review scientific journal.

2.5 Biota

2.5.1 Bivalves

So far, most studies on MP identification in biota have been done using FTIR analysis. Some few studies employed LDIR, typically considering totally-reflective slides, which require additional sample preparation steps (e.g., evaporation, aliquoting, etc.) increasing the risk of MP loss and deceptive extrapolations. To address these limitations, UDC and BfG independently developed a transfer protocol from stainless-steel filters (10 µm) to gold-coated filters (0.8 µm), enabling reliable measurements using a quantum-cascade laser-based infrared transflectance system (QCL-LDIR) without the need for withdraw aliquots. This approach requires effective digestion protocols to prevent filter clogging, requiring careful optimization of experimental conditions.

At UDC, several digestion protocols for bivalves, using mussels as an exemplary matrix were developed and validated for MP determination. These included alkaline, oxidative, and enzymatic approaches, and some of their combinations. The enzymatic-oxidative protocol demonstrated the highest digestion efficiency. However, a modified two-step alkaline oxidation combined with a surfactant provides a cost-effective and faster alternative, though it involves two filtration steps, which can increase the risk of MP loss. The gold-coated filter transfer approach was validated against a Syncore multi-sample automatic evaporation system previously employed (López-Rosales et al., 2022). The enzymatic-oxidative digestion followed by a total transference of the suspension to gold-coated filters achieved the highest recovery rates for most polymers: 90–97 % for PET (fibers), PVC, PS, PET, PP, PA, and PE. A manuscript detailing the methodology and results for mussels has been submitted to the peer-reviewed scientific journal *Marine Pollution Bulletin*.

This newly developed analytical method was applied to clams from the North Sea (GEOMAR), invasive Red Swamp crayfishes and clams from the Mero-Barcés River basin (UDC) to quantify and characterize MPs (20–5000 µm) in these samples, alongside blank procedures.

The clams collected from the North Sea were preserved in formalin. However, none of the MP extraction methods proved to be satisfactory, likely due to the preservation method used. Formalin preservation is not recommended for MP analysis as it requires extensive washing to fully remove the preservative agent and enable efficient matrix digestion and MP extraction. Additionally, this preservation method has been reported to negatively affect specimen tissues (Ilechukwu et al., 2023). To ensure reliable MP analysis, it is advisable to freeze collected individuals immediately after their sampling.

Following this recommendation, the clams collected from the Mero-Barcés Reservoir were frozen at -20 ºC after collection and digested successfully using the enzymatic-oxidative protocol shown in **Error! Reference source not found.**. A pooled sample of 16.2 g from 26 individuals was processed and analysed by LDIR. The MP concentration was determined to be 6 MPs/g, with a total of 5 particles and 1 PET fibre per individual, corresponding to approximately 598.8 MPs per 100 g and an average of 3.73 MPs per individual. Among the identified polymers, PP and PET were the most abundant ones (24 % each), together accounting for nearly half of the total MPs detected, followed by PA (16 %), PU (10 %), PE (7 %) and rubber (4 %). The size distribution analysis revealed that 62 % of the particles fell within the 50–20 µm range, indicating a higher retention of smaller MPs and particles.

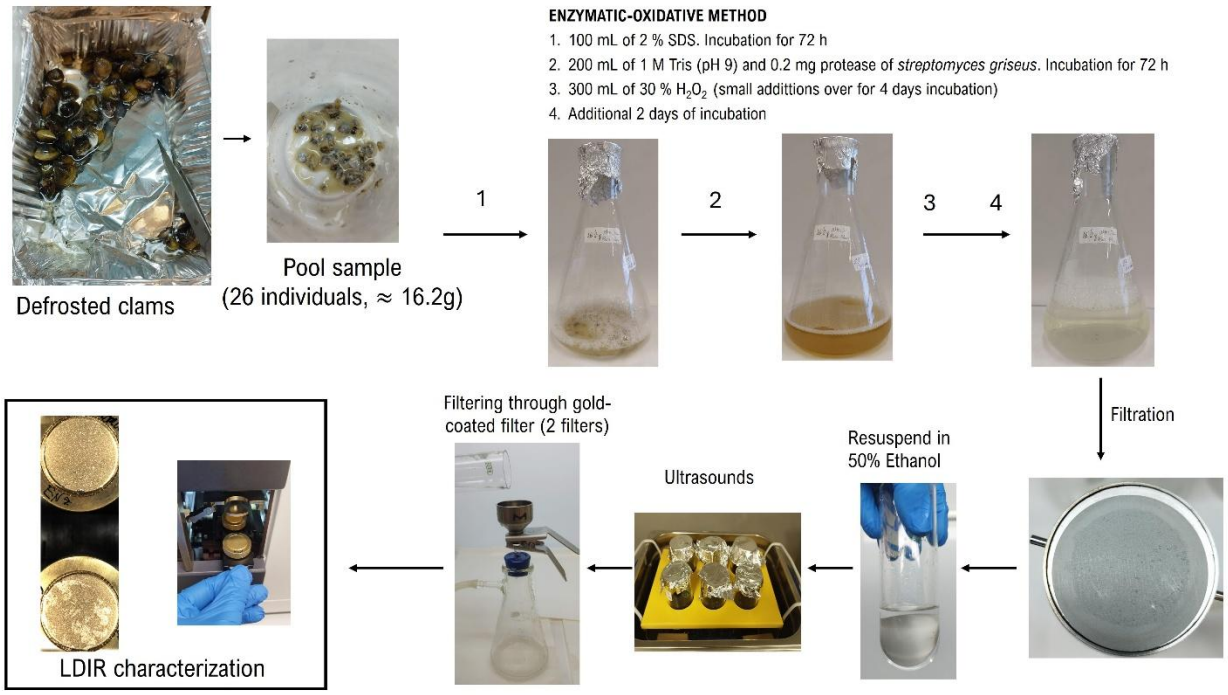

Figure 15: Scheme of the sample treatment process for MP characterised in clams using the enzymatic-oxidative method, including the transfer protocol to gold-coated filters before LDIR analysis.

The MP analysis of invasive Red Swamp crayfish (approx. 10-15 cm long) was collected at the Mero-Barcés (see Deliverables D2.3 and D2.4 for further information). However, in this case, gastrointestinal tracts from 72 individuals were extracted (34 g in total), yielding three aliquots of 12.1 g, 12.7 g and 9.2 g. Only the data from the first aliquot (12.1 g) are presented here. The enzymatic-oxidative method, based on 2 % SDS and 30 % H_2O_2 was applied (Figure 15). It is worth noting that up to four gold-coated filters were required for LDIR analysis (20–5000 µm), as opposed to the two filters required for the clam sample, revealing that crayfish retained many particles in their gastrointestinal tracts.

Overall, the crayfish showed MP ingestion, with nearly 6 MPs/g detected in the gastrointestinal tract, corresponding to approximately 4.5 MPs per individual. When extrapolated to the number of individuals, this corresponds to approximately 4.5 MPs per crab. The predominant polymers in this sample were PS and PET. The possible sources of PS remain unknown, as this polymer was not dominant in other analysed samples from the Mero-Barcés (e.g. clams, water). Therefore, further evaluation of the remaining aliquots of the crayfish sample is necessary to determine the consistency of these results.

2.6 Atmospheric deposition

2.6.1 Atmospheric deposition – sample treatment and data overview

A schematic representation of the processing and analysis workflow for atmospheric deposition samples from the Mero-Barcés River basin and Thames River at UDC is shown in Figure 16. The methodology includes a low-to-moderate digestion protocol (SDS and H_2O_2) as described in Deliverable D3.2 and published by López-Rosales et al. (2024). The treated samples and blank procedures were analysed by LDIR (20-5000 µm) with a hit quality index (HQI) threshold of 0.90 (0.95 for rubber particles). A transfer protocol from stainless-steel filters to gold-coated ones, required for transflectance measurements using a QCL-LDIR system, was implemented. This new approach enhances MP recovery rates, particularly for fibers, as gold-coated filters improve detection efficiency.

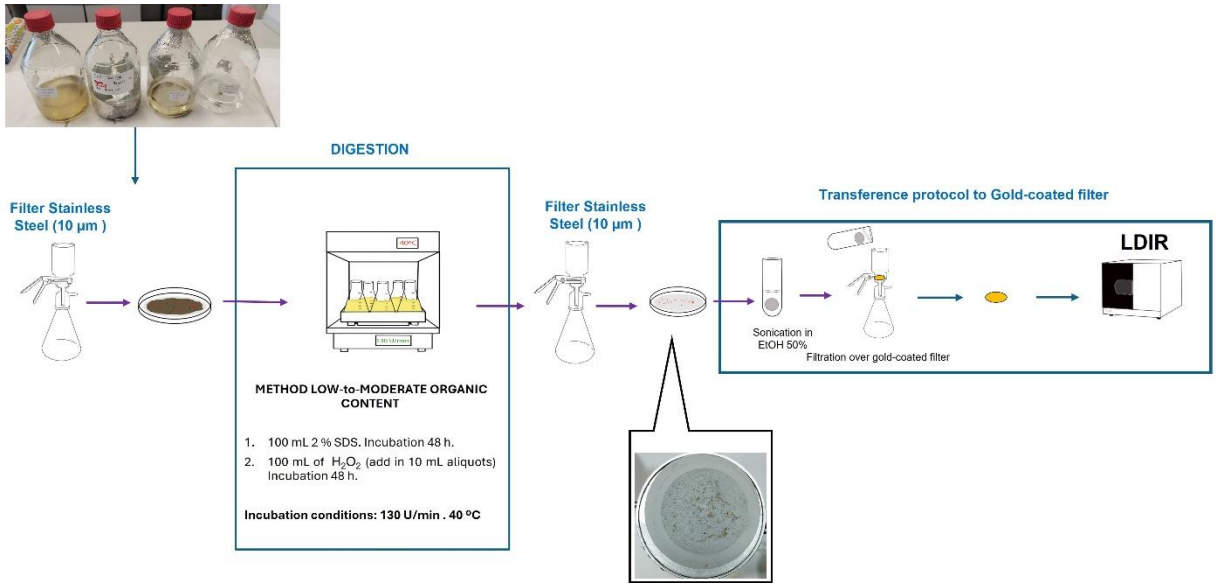

Figure 16: Methodology for MPs analysis in atmospheric deposition samples at UDC.

Data on MP abundance and polymer types from the Mero-Barcés basin are presented in Figure 17 and Figure 18. Results from the first two sampling campaigns of Year 2 (winter and spring 2023) were included in Deliverable D2.4. Data from atmospheric deposition samples collected during summer and autumn 2023 are presented here, alongside a comparative analysis of results from Years 1 and 2.

Additionally, samples from the Elbe River, collected and analyzed by BfG, are also presented (Figure 19 and Figure 20), along with atmospheric samples from the Thames River, collected by NOC in 2023 and processed at UDC (Figure 21 and Figure 22).

2.6.2 Atmospheric deposition in the Mero-Barcés case study

The abundance of MPs (by particle number) and polymer types identified in samples from summer and autumn 2023 (Year 2) are shown in Figure 17. Two passive sampling devices were employed to collect atmospheric bulk deposition (wet and dry deposition), namely EnviroPlaNet, a prototype from the Spanish Network of Researchers working on plastic pollution (www.enviroplanet.net), and the commercial Depobulk® system.

In summer 2023, the Depobulk® system recorded an average deposition rate of 275 ± 64 MPs/m²/day, while the EnviroPlaNet sampler measured a higher average rate of 516 ± 134 MPs/m²/day. During autumn 2023, both systems recorded lower MP deposition rates: 168 ± 43 MPs/m²/day for Depobulk® and 354 ± 94 MPs/m²/day for EnviroPlaNet. Figure 17 shows the average of 2 replicates using both passive samplers, classified by shape (fibre or particle), size and polymer type.

Both samplers consistently showed that the majority of MPs collected were in the smallest size range (50–20 µm) as particles, whereas fibres were predominantly in the larger size ranges (> 50 µm). For Depobulk®, MPs within the 50–20 µm range accounted for approximately 78 % of total particles in summer and 68 % in autumn, while for EnviroPlaNet, this proportion increased to 87 % in summer and 66 % in autumn. Fibers ranged from 3 to 8 %.

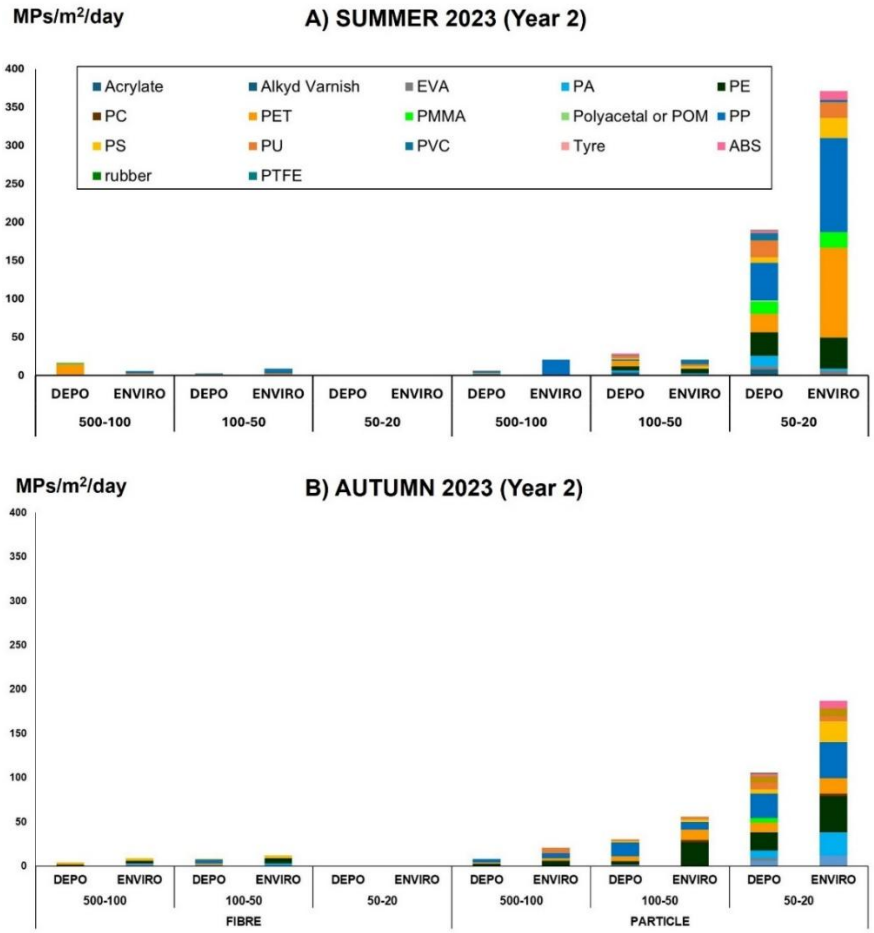

Figure 17: Average deposition rates (MP/m²/day) of airborne MP (n = 2) using the two sampling devices classified by shape (fibre or particle), size (µm) and polymer type. A) 2nd year (2023) summer sampling campaign and B) autumn 2023 sampling. 'Depo' and 'Enviro" stand for the Depobulk® and EnviroPlaNet systems, respectively.

Table 1 summarizes the percentages of different polymer types found during atmospheric deposition campaigns conducted in the summer and autumn of 2023, using the two samplers (Depobulk® and EnviroPlaNet). Results are reported for the total range of microplastics (MPs) collected (particles and fibers) and specifically for the most abundant size fraction (20–50 µm).

In the summer of 2023, the analysis of airborne MPs detected by the Depobulk® and EnviroPlaNet samplers highlighted PP as the dominant polymer in both total particles (fibers and particles) and the 20–50 µm size range. The Depobulk® sampler recorded 22.7 % PP in total particles and fibers, increasing to 25.8 % within the 20–50 µm particle range, followed by PET (19.4 % total; 12.7 % in the 20–50 µm range) and PE (14.9 % total; 16.2% in the 20–50 µm range). In contrast, the EnviroPlaNet sampler exhibited higher proportions of PP (34.9 % total; 33.1 % in the 20–50 µm range) and PET (28.8 % total; 31.5 % in the 20–50 µm range), with PE showing similar levels (11.0 % total and in in the 20–50 µm range).

In autumn 2023, a seasonal shift was observed. The Depobulk® sampler recorded a sharp increase in PP levels to 33.0 % (total particles and fibers) and 26.4 % in the 20–50 µm range, accompanied by a rise in PE (17.9 % total; 19.4 % in the 20–50 µm range) and a drop in PET (13.7 % total; 10.4 % in the 20–50 µm range). The EnviroPlaNet sampler, on the other hand, detected a significant increase in PE (28.9 % total; 21.9 % in the 20–50 µm range) and PS (11.3 % total; 12.5 % in the 20–50 µm range), with PP levels dropping to 19.6 % (total) and 21.9 % (20–50 µm range).

Table 1: Percentage of airborne MPs (total range and the most abundant size fraction) by polymer type detected using Depobulk® and EnviroPlaNet samplers in summer and autumn 2023

	% Airborne MPs (PARTICLES AND FIBERS)				% Airborne MPs (20-50 µm, PARTICLES)			
	Summer 2023		Autumn 2023		Summer 2023		Autumn 2023	
Polymer Type	**Depobulk®**	**EnviroPlaNet**	**Depobulk®**	**EnviroPlaNet**	**Depobulk®**	**EnviroPlaNet**	**Depobulk®**	**EnviroPlaNet**
Acrylate	4.2	0.0	3.3	5.2	3.5	0.0	3.5	6.3
Alkyd Varnish	1.2	0.0	2.4	0.0	0.8	0.0	2.1	0.0
EVA	2.1	1.4	1.9	0.0	1.9	1.6	2.8	0.0
PA	6.9	1.4	5.7	10.3	7.3	0.8	8.3	14.1
PE	14.9	11.0	17.9	28.9	16.2	11.0	19.4	21.9
PC	0.0	0.0	0.0	2.1	0.0	0.0	0.0	1.6
PET	19.4	28.8	13.7	11.3	12.7	31.5	10.4	9.4
PMMA	6.9	4.8	3.3	0.0	8.5	5.5	4.9	0.0
POM	0.6	0.0	0.0	0.0	0.8	0.0	0.0	0.0
PP	22.7	34.9	33.0	19.6	25.8	33.1	26.4	21.9
PS	3.9	6.8	4.7	11.3	3.8	7.1	4.9	12.5
PU	10.4	5.5	6.1	5.2	11.5	5.5	6.9	3.1
PVC	4.2	2.7	5.7	3.1	5.0	0.8	6.9	4.7
Tyre	0.0	0.0	0.0	0.0	0.0	0.0	0.0	0.0
ABS	2.4	2.7	1.9	3.1	1.9	3.1	2.8	4.7
Rubber	0.3	0.0	0.5	0.0	0.4	0.0	0.7	0.0
PTFE	0.0	0.0	0.0	0.0	0.0	0.0	0.0	0.0

Other notable findings included the consistent presence of PU (ranging between 3.1 % and 11.5 % across samplers and size ranges), a slight increase in PA during autumn (notably reaching 14.1 % in the 20–50 µm range for the EnviroPlaNet sampler), and the absence of materials such as tyre particles and PTFE across all campaigns. Acrylates and PMMA showed variable levels, with a general reduction from summer to autumn.

Both samplers identified PP, PE, and PET as predominant polymers, but their proportions differed significantly depending on the sampler and season. The higher PET levels detected by EnviroPlaNet in summer and the increase in PE and PS in autumn point to possible differences in sampler design and collection efficiency, already mentioned in Deliverable D2.4.

A comparative analysis of atmospheric deposition results from Year 1 (summer 2021 - winter 2022) and Year 2 (winter 2023 - autumn 2023) from Mero-Barcés is shown in Figure 18, based on averages and 95 % confidence intervals (X ± 2SD). As outlined in Deliverable D2.4, the EnviroPlaNet sampler generally yielded higher deposition values than the Depobulk® system, although these differences were statistically significant only in autumn 2021. The Depobulk® sampler displayed lower data dispersion, likely due to its larger collection surface, while EnviroPlaNet exhibited greater variability and occasional overrepresentation, particularly in certain campaigns.

In both years, the majority of MPs were within the 50-20 µm size range, with proportions increasing from autumn to spring. This pattern likely reflects seasonal changes in MP sources or atmospheric processes affecting their transport and deposition. The improved methodological protocols introduced in Year 2 enhanced the resolution of size-specific distributions compared to Year 1.

The observed differences between sampling devices and across seasons highlight the importance of considering sampler design and environmental factors when conducting atmospheric deposition studies.

Figure 18: Atmospheric deposition data comparison of sampling campaigns from the 1st and 2nd years from Mero-Barcés. Average ± SD (green) and average ± 2SD (yellow) of total MP deposition (MP/m²/day) encountered for each sampling device in each sampling month (n = 2).

2.6.3 Atmospheric deposition in the Elbe River case study

Atmospheric samples from Hamburg (sites Altona and Veddel) were analysed by LDIR at BfG using Kevley (low-e IR reflective) slides. The measured spectra were compared to an in-house reference library. For analysis, all spectra with an HQI > 0.80 (rubber > 0.90, PA and PE-Cl > 0.85) were included.

A procedural blank was prepared in the laboratory of the German Federal Institute of Hydrology, which contained 1 PC and 1 POM. The results, shown in Figure 19, indicate that the MP concentrations in Veddel (east of the harbour) were higher than in Altona (north of the harbour). In Altona, MP counts ranged from a minimum of 54 MPs over 14 days to a maximum of 223, whereas in Veddel, values ranged from 61 MPs to a maximum of 874 MPs. A general rise in MP concentrations was observed in Altona from winter to autumn, while in Veddel, this opposite trend was noted. This pattern is likely influenced by wind direction, though further analysis is required for confirmation.

The polymer composition varied across samples, with high levels of Acrylates/PU/Varnish and Acrylonitrile butadiene present in all samples. PVC exhibited the highest concentration in both sampling sites during summer. PS, PC and EVA were found in low amounts and were not present in all samples, with PS appearing only in summer and autumn. PTFE and rubber reached their highest levels in winter at Veddel. However, no clear seasonal trend was observed overall.

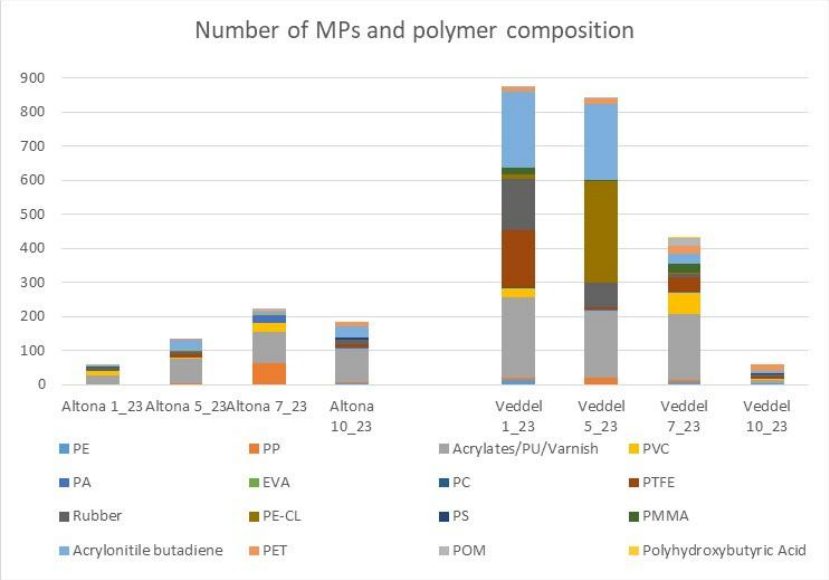

Figure 19: Number of MPs (total in 14 days) and polymer composition in the atmospheric samples from Hamburg in the Elba River.

Regarding the size (Figure 20), the 10-50 µm fraction constitutes the main contributor to the total atmospheric deposition of MPs (60-90 %). In contrast, only very few MPs with a size of 300-1000 µm were detected.

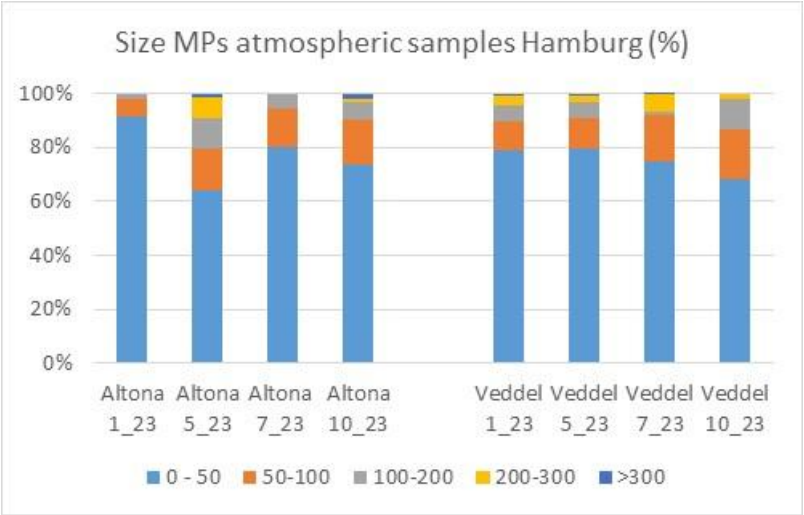

Figure 20: Size distribution in atmospheric samples from Hamburg in the Elba River.

2.6.4 Atmospheric deposition in the Thames River case study

Atmospheric deposition samples from the 2023 season campaign were collected by NOC from two sites along the Thames River: Brentford Barge (51.480°N, 0.303°E) and Erith Barge (51.504°N, 0.168°E). Two sampling campaigns, each lasting approximately 1.5 months, were conducted from July-August (04/07/2023–14/08/2023) and August-September (14/08/2023-18/09/2023) using air passive samplers (conical funnel: 12 cm diameter, 11 cm total height including the stem).

All deposition samples from the Thames River were processed at UDC using the low-to-moderate digestion protocol (see Figure 16), following the same protocol described for the Mero-Barcés samples.

As shown in Figure 21, LDIR analysis of the first sampling campaign (July–August 2023) at the Thames River indicates minor differences in total MP deposition rates between Brentford Barge (1464.3 MPs/day/m², Figure 21A) and Erith Barge (1265.9 MPs/day/m², Figure 21B). However, polymer composition varied between sites, with PE (50–20 µm) as the dominant polymer at both locations. At Brentford Barge, PS was the second most prevalent polymer, whereas at Erith Barge, ABS was the second most dominant polymer, while overall PE levels remained similar at both sites.

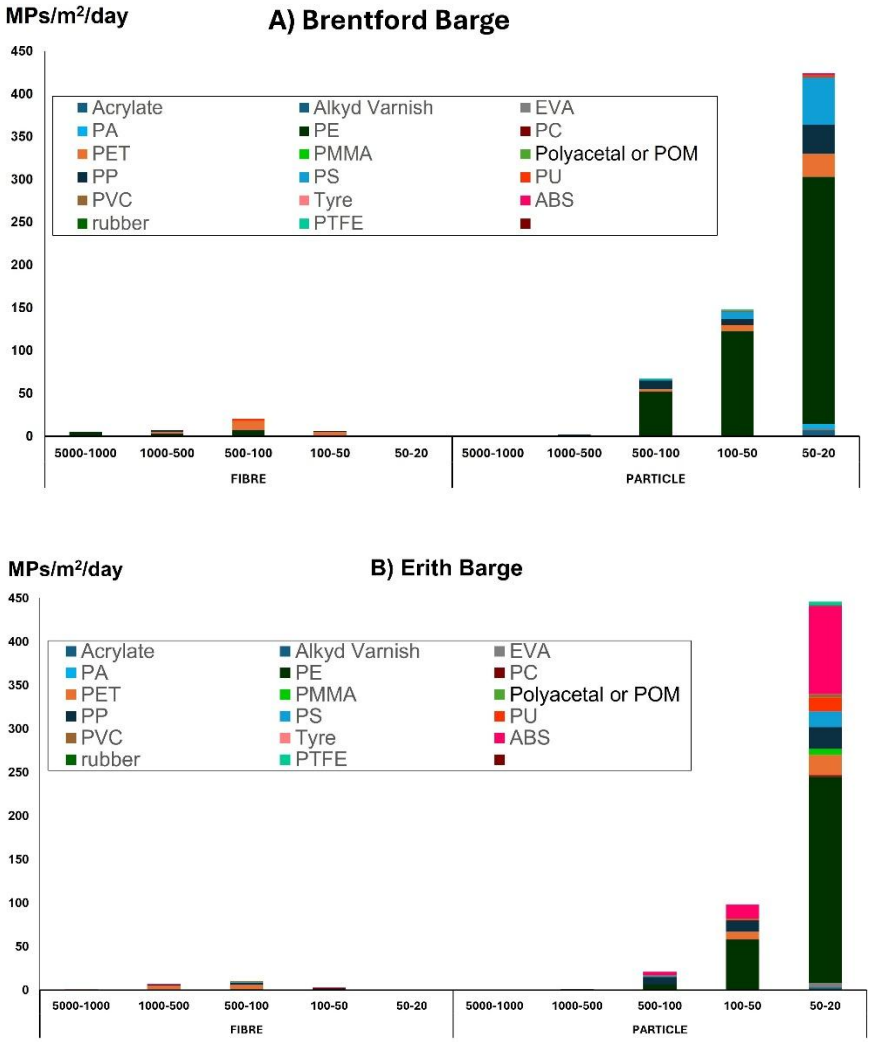

Figure 21: Average deposition rates (MP/m²/day) of airborne MPs from the first sampling campaign at the Thames River classified, by shape (fibre or particle), size (µm), and polymer type: A) Brentford Barge and B) Erith Barge.

In contrast, the second sampling campaign (August–September 2023) revealed more pronounced differences, with Brentford Barge showing a deposition rate of 1152 MPs/day/m², compared to 601.3 MPs/day/m² at Erith Barge (Figure 22). Polymer distribution also differed between the two sites: PS remained the dominant polymer at Brentford Barge, followed by PE and PP, whereas at Erith Barge, PE and PP were the most abundant, with a more even distribution across polymer types.

These variations in deposition rates and polymer composition highlight differences between the two locations at the Thames River over time. Further analysis considering meteorological conditions, potential emission sources, and site-specific influences may help contextualize these observations.

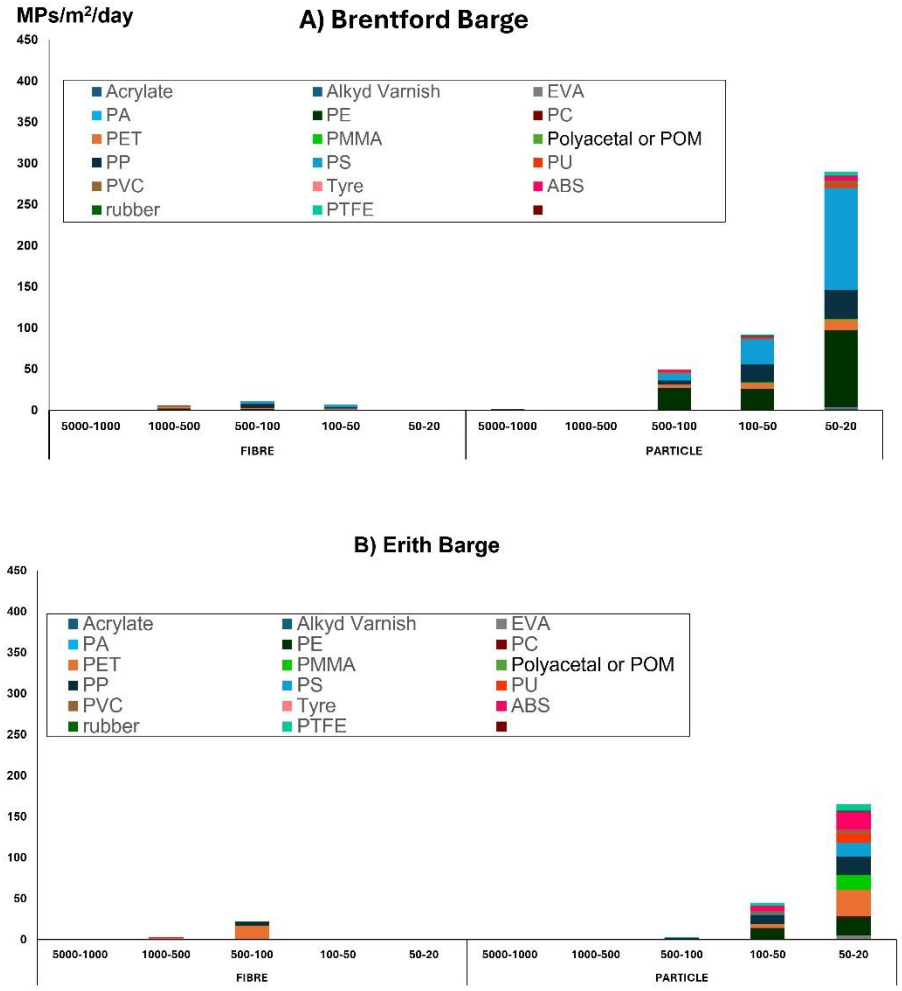

Figure 22: Average deposition rates (MP/m²/day) of airborne MP from the second sampling campaigns at the Thames River classified by shape (fibre or particle), size (µm) and polymer type. A) Brendford Barge and B) Erith Barge.

3 RESULTS OF THE CHARACTERIZATION OF MP EMISSIONS FROM ROAD DUST AND WATER RUN-OFF IN THE MERO-BARCÉS CASE STUDY

To characterise the land-based sources (Subtask 3.3.2) and determine the contribution of MPs to the environment, sampling sites of the Mero-Barcés case study have been selected, with special interest in the Cecebre reservoir, for stormwater runoff corresponding to a motorway toll (20,000 - 25,000 vehicles/day) and treated urban wastewater sampling corresponding to a waste-water treatment plant (WWTP), discharging to the Mero River.

3.1 Waste-water treatment plant (WWTP)

Two sample effluents from the WWTP EDAR, located near the Mero-Barcés Reservoir, were collected during two separate sampling events: sampling 1 (09/10/2023) and sampling 2 (16/10/2023).

To complement the characterization of the WWTP samples analysed by pyrolysis-gas chromatography-mass spectrometry (Py-GC-MS) to quantify MP content by mass (results presented in Deliverable D3.3), a detailed analysis of the MPs was performed using LDIR at UDC.

All WWTP samples were processed at UDC using the low-to-moderate digestion protocol (see Figure 16), which follows the same procedure as that used for atmospheric deposition samples. Sample 1 (first sampling) involved filtering 12.6 liters of water, resulting in a MP concentration of 20.2 MPs per liter (20159 MPs/m³, Figure 23A). Sample 2 (second sampling) involved filtering 9.6 litres of water, yielding 41.6 MPs per litre (41520 MPs/m³, Figure 23B). These results demonstrate notable differences in the number of MPs present in the samples over just a 7-day interval. However, in both samplings, the predominant polymers detected were PP (46 % and 35 %, respectively), followed by PET (25 and 40 %, respectively). Among the fibers detected, PET was the dominant polymer, suggesting that PP and PET are the most frequently released polymers from the local WWTP into the environment.

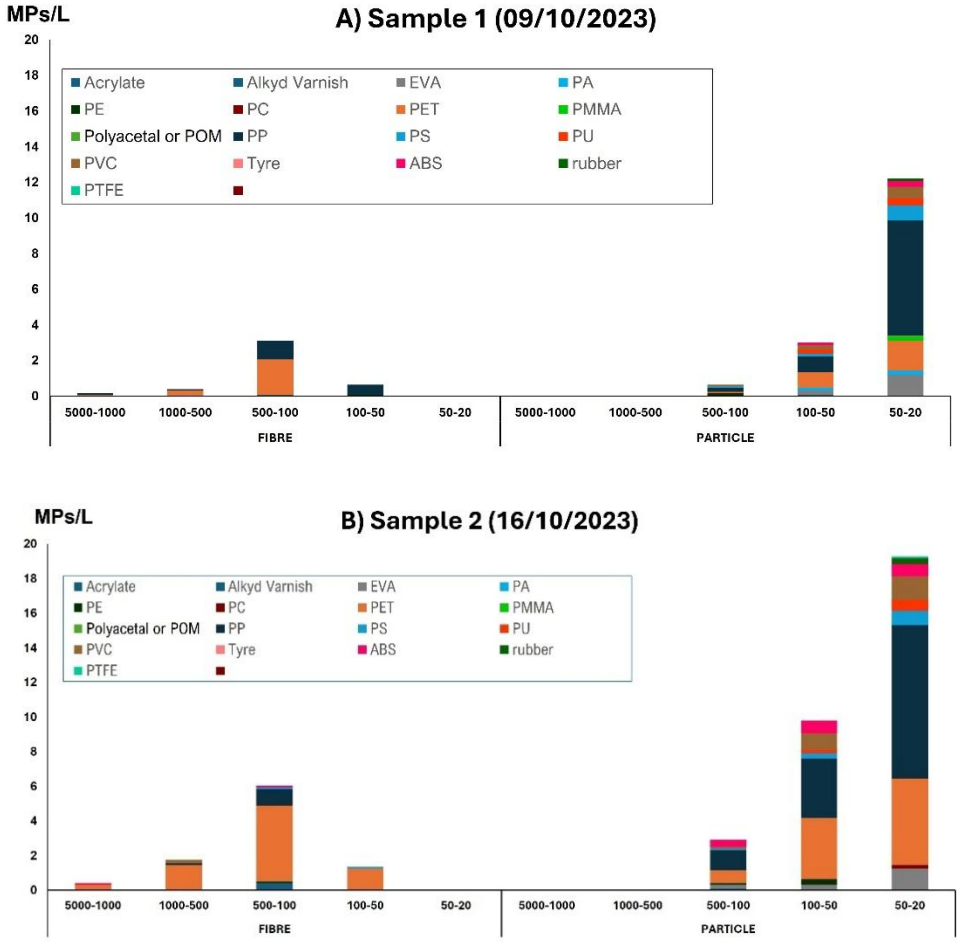

Figure 23: Average MP content (MP/L) of WWTP samples from the Mero-Barcés case study classified by shape (fibre or particle), size (µm) and polymer type. A) Sample 1 (collected 09/10/2023) and B) Sample 2 (16/10/2023).

Py-GC-MS analysis of the two WWTP samples (see Deliverable D3.3 for further details) revealed that PET contributed the highest concentration, followed by SBR and PA 6. When comparing LDIR results with Py-GC-MS data, a strong correlation was observed for PET, indicating that both methods consistently identified this polymer. However, no significant or no detectable MPs from tyres were found in either sample using LDIR, which highlights the capability of Py-GC-MS to detect tyre-related markers, such as SBR. On the other hand, PP was below the limit of quantification for Py-GC-MS in sample 1, while it was identified as the most abundant polymer by LDIR. It is important to note that the volume analysed by Py-GCMS was between 50-100 mL, whereas for LDIR, approximately 10 L of sample were used. This highlights the need for complementary MP

analysis techniques, such as LDIR (which is number-based) and Py-GC-MS (which is mass-based), to provide a more comprehensive understanding of the sample.

3.2 Road dust

The proposed methodology, validated and proved with road dust samples (Deliverable D3.3), has been applied to analyse samples collected at a national highway toll (AP 9) of both road dust and water runoff and thoroughly analysed for MP and plastic additives.

The collection of road dust samples (RDS) has been carried out manually and by means of sweeping/sweeping, it is carried out at the Cecebre Toll, located at kilometre point 15.4 of the AP-9 motorway (*Autopista del Atlántico*), in the vicinity of the Abegondo-Cecebre reservoir (Figure 24). The pavement of the AP-9 motorway on the specific section of the toll is concrete, as an exception to the asphalt pavement of the AP-9 motorway. The AP-9's DTI on this section is around 24,000 vehicles/day, of which approximately 10 % are heavy vehicles.

Figure 24: Image of the access to the Cecebre toll (km 15.4 of the AP-9 towards A Coruña), with lanes 2 (telepayment) and 3 (manual payment), numbered from the left, showing the transition from asphalt agglomerate pavement to concrete pavement in the toll section (Source: Google Maps).

The RDS are collected in three different areas of the toll: two located along lanes 2 and 3, and a third in an area of 1 m^2 delimited between the two lanes, in an area of asphalt pavement, outside the toll shelter, which has been called 'island'.

Both sweeping/ vacuuming and manual collection of RDS are always carried out in the same three areas to assess the accumulation of RDS over time. Sweeps/ vacuuming of lanes 2 and 3 are always carried out in the sections of the toll lanes that are covered by the shelter from direct rain. The island, on the other hand, is in an area exposed to the elements.

Toll lane 2 operates by remote payment, while lane 3 is a conventional payment lane at the toll booth. These characteristic conditions the different behaviour of the vehicles crossing them in terms of braking and acceleration behaviour. It is hypothesised that this aspect may be reflected in the characteristics of the RDS accumulated on the respective lanes.

3.2.1 Sampling of motorway road dust

The sweeping/ vacuuming of RDS on lanes 2 (V2, Remote payment) and 3 (V3, Manual payment) is carried out on 8 m long by 0.4 m wide strips (Figure 25), delimited on both sides of each track (total swept/ vacuumed surface: 6.4 m2 on each lane). As mentioned above, sweeping/ vacuuming on the 'island' (V1V2) is carried out on a rectangular area of 0.5 x 2 m.

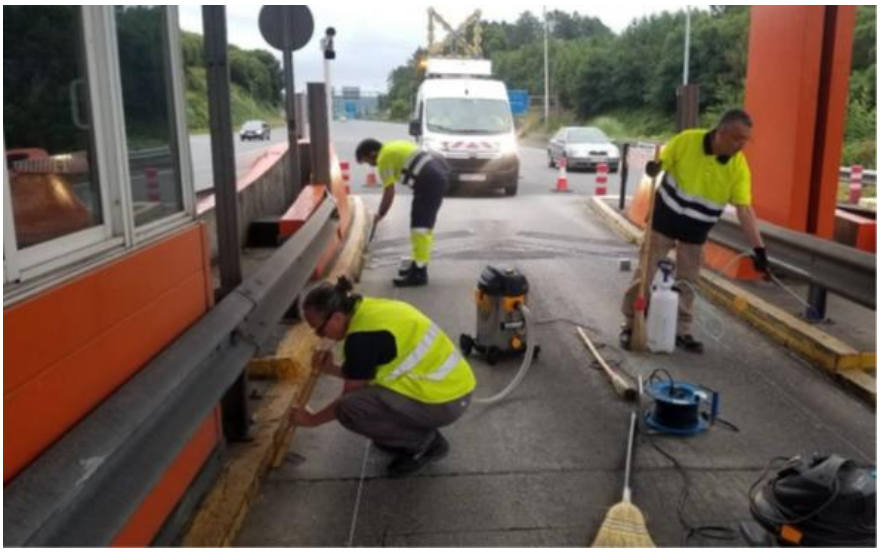

Figure 25: Development of sweeping/ vacuuming operations on lane 2 of the AP9 toll station at Cecebre.

The collection of road sediments was carried out following the usual recommendations to preserve the samples from contamination by microplastics, although subject to the safety measures required by the motorway concession company to allow access to the toll facilities in terms of clothing (high-visibility clothing and safety footwear).

The sweeping/ vacuuming zones were marked with hemp ropes, and driving on these ropes during sweeping/suction operations was avoided. However, it should be noted that the toll staff, wearing the appropriate safety clothing, are constantly moving around the toll lanes.

Sweeping of sediment was carried out with brooms, brushes and brushes made of plant materials. Trowels, spatulas and stainless-steel scoops were also used for manual collection. The manually collected road sediments were deposited directly into glass containers with an aluminium foil seal.

For sediment collection by suction, an industrial hoover with a stainless-steel tank was used, replacing the metal suction tube with a specially designed one made of bamboo cane.

3.2.2 Results of motorway road dust

The sampling campaigns consisted of three sweeps conducted in 2024 to analyse different sediment fractions under varying climatic conditions. Sweep 0 (B0) took place in April 2024, focusing on sediment particles smaller than 1 mm. Sweep 1 (B1) was carried out in July 2024, expanding the analysis to include three size fractions: particles smaller than 1 mm, 250 µm, and 63 µm. Similarly, Sweep 2 (B2), conducted in October 2024, followed the same methodology as Sweep 1, examining sediment fractions below 1 mm, 250 µm, and 63 µm. In addition, road dust collected during the second campaign (B1) was sent to UVigo for ecotoxicological studies (WP6, see further details in Deliverable D6.4).

Analysis of MPs in the motorway road dust samples by thermoanalytical techniques

The quantitative analysis of ten microplastic (MP) types in the road dust samples collected at the AP9 toll station is summarized in Table 2. Pyrolysis-GC-MS analysis revealed that road dust samples from the manual toll lane exhibited the highest MP concentrations, with levels detected in the ppm range (μg g^{-1}) or higher. Among the ten quantified MPs, styrene-butadiene rubber (SBR) and acrylonitrile-butadiene-styrene (ABS) were the most abundant, both of which are also recognized potential tyre wear markers. Smaller particle sizes (< 63 μm and < 250 μm) showed higher concentrations of specific polymers such as SBR, ABS, and PMMA, indicating that finer road dust fractions are more enriched with MPs due to their ability to retain smaller particles.

Table 2: Quantitative analysis of MPs in the three samples of road dust (A) Sweep B0, B) Sweep B1 and C) Sweep B2) taken at the AP9 toll station by Py-GC-MS.

A)

	SWEEP B0		
μg g^{-1}	**B0-V1V2**	**B0-V2**	**B0-V3**
PS	244.7	143.7	254.7
SBR	59.36	1053	3392
PET	15.83	23.34	18.31
PMMA	183.3	102.7	181.7
PC	0.15	1.97	2.59
PA 6	13.30	26.88	110.0
PE	95.19	105.3	301.4
PP	18.51	52.09	1335
ABS	60.35	285.5	513.9
PA 6,6	92.60	127.5	513.9
Total	783	1922	6624

B)

	B1					
μg g^{-1}	**B1V2 < 63 μm**	**B1V2 < 250 μm**	**B1-V2 < 1 mm**	**B1V3 < 63 μm**	**B1V3 < 250 μm**	**B1-V3 < 1 mm**
PS	226.7	184.0	140.5	345.9	310.4	340.1
SBR	6877	6861	1793	7179	9823	3846
PET	145.8	74.87	54.39	390.4	280.2	71.98
PMMA	464.5	428.4	57.79	516.5	610.3	80.55
PC	9.15	10.36	5.22	11.62	5.08	2.04
PA 6	146.8	124.7	48.24	247.1	197.5	70.42
PE	504.5	477.2	235.0	534.2	436.1	240.2
PP	165.8	94.75	62.55	213.4	142.9	87.52
ABS	2912	1781	283.2	2800	3204	804.9
PA 6,6	578.8	415.3	194.8	633.9	486.0	303.0
Total	12032	10452	2875	12871	15496	5847

C)

	B2					
µg g^{-1}	B2V2 < 63 µm	B2V2 < 250 µm	B2V2 < 1 mm	B2V3 < 63 µm	B2V3 < 250 µm	B2V3 < 1 mm
PS	235.1	200.4	171.4	378.4	372.8	399.9
SBR	5808	5157	3965	6835	7754	5895
PET	72.98	45.51	120.5	131.9	142.0	68.47
PMMA	327.0	345.4	321.9	293.7	270.7	777.0
PC	5.23	7.14	5.12	6.99	7.59	6.16
PA 6	145.7	100.7	108.5	231.4	223.1	177.2
PE	602.3	464.5	395.1	579.8	613.9	506.3
PP	55.7	56.7	34.5	60.0	38.1	37.1
ABS	3243	2289	2101	4327	2434	2536
PA 6,6	327.5	428.0	463.7	773.3	740.7	603.9
Total	10823	9094	7687	13618	12597	11006

Additionally, qualitative TD/Py-GC-MS analysis was performed to identify organic contaminants and plastic additives in the samples. This analysis detected tyre-specific compounds, including styrene, N-Phenyl-N'-(1,3-dimethylbutyl)-p-phenylenediamine (6PPD)—a rubber industry antioxidant and anti-ozonant (Ihenetu et al., 2024)—and dipentene, a product of tyre pyrolysis. Furthermore, polycyclic aromatic hydrocarbons (PAHs) characteristic of asphalt were also identified.

Analysis of plastic additives in road dust samples by GC-MS/MS

A method for the analysis of 50 plastic additives using sonication extraction with dispersive solid-phase extraction (SPE) clean-up and GC-MS/MS determination was developed and validated (see Figure 26). The method demonstrated good accuracy, with recoveries ranging from 73 % and 137 %, and good precision (RDS < 20 %) for all additives.

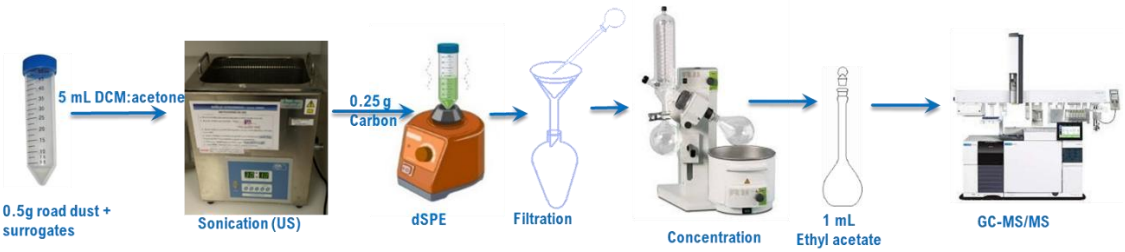

Figure 26: Schematic representation of the method for the analysis of plastic additives by GC-MS/MS.

Samples of three particle sizes (< 1mm, < 250µm and < 63µm) from both road dust sampling periods in the Mero-Barcés area - B1 (July 2024) and B2 (October 2024) - were analysed. Small differences were observed between particle size fractions (< 1 mm and < 63 µm fractions, presented in Figure 27).

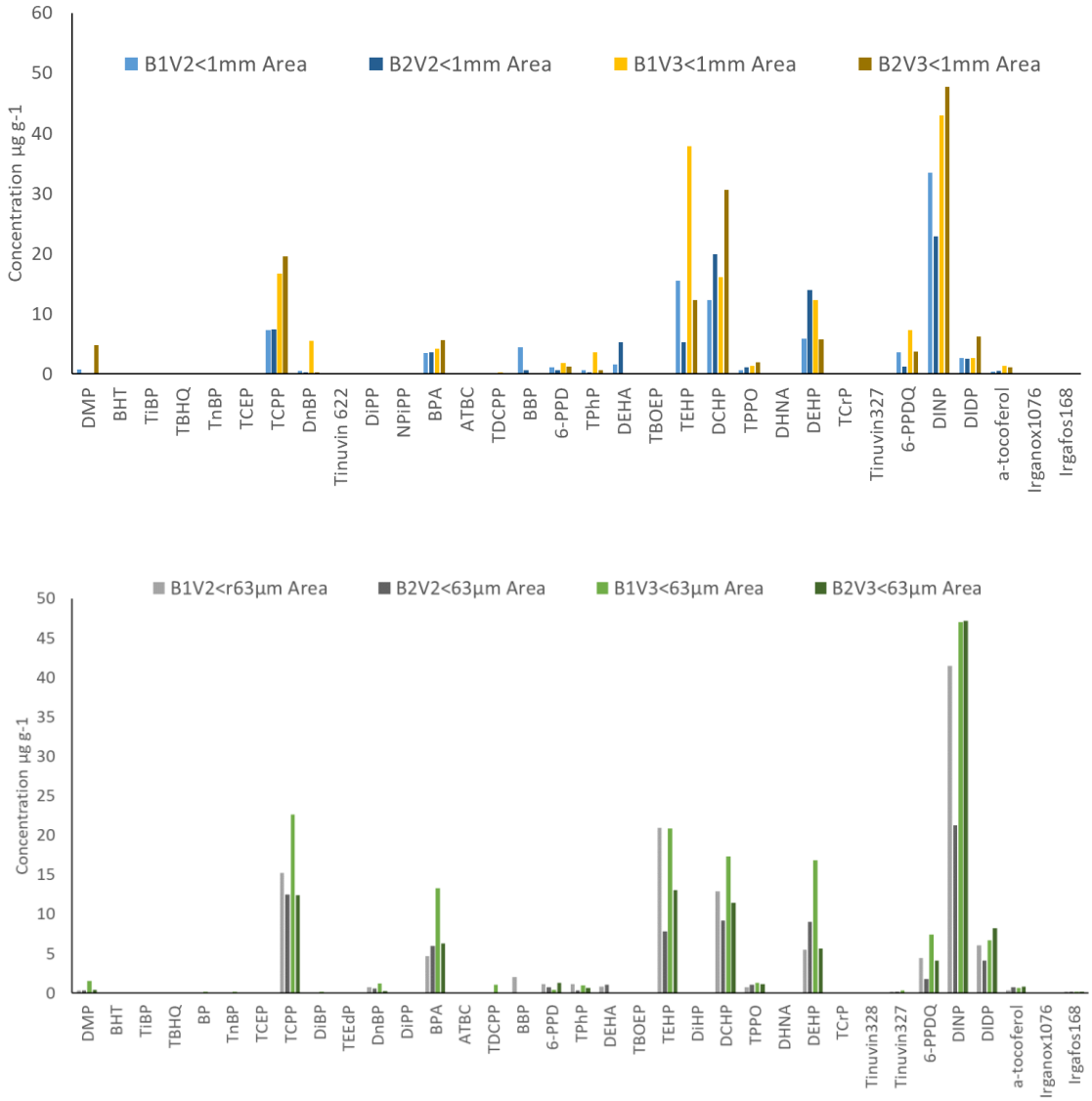

Figure 27: Quantitative analysis of 50 plastic additives in motorway road dust samples by GC-MS/MS.

As shown in Figure 27, higher concentrations of additives were detected in the manually operated lane (V3) compared to the remote payment lane (V2). The compound profiles from both sampling periods were very similar. The main additives detected across all samples were plasticizers (e.g. DCHP, DEHP, DINP, DIDP, BPA; see further details in Deliverable D4.6 Annexes) and flame retardants (e.g.TCPP and TEHP), with concentrations ranging from 5 to 41 µg g^{-1}. Additionally, 6-PPD and its quinone derivative, 6-PPDQ (Ihenetu et al., 2024), were detected at concentrations between 0.5 and 8 µg g^{-1}. Phthalates (DiPP, DiBP) and benzophenone (BP, a UV filter) were only found in the smaller particle fractions (< 250 µm and < 63 µm).

3.3 Water Runoff

3.3.1 Sampling of motorway water runoff

A first sampling of runoff water on the AP9 motorway has been performed and analysed during two different rainfall events. Twenty-four samples were collected over the total duration of each event. A sampling station

with a flowmeter, rain gauge and sampling equipment from the control section connected to the rainwater well has been installed to monitor runoff from the highway close to the Toll Station (Figure 28).

Figure 28: Stormwater sampling station with monitoring equipment, flowmeter, data loggers and power supply batteries

3.3.2 Results of motorway water runoff

The filters analysed correspond to 3 samples selected from each of the events after being filtered through 1 µm pore size glass fibre filters (Table 3). Some samples, especially the first aliquots collected from one of the events, showed unusually high conductivity values. It was confirmed that this is caused by high concentrations of chlorides which may originate from the salt used when de-icing of the roadway is required.

Table 3: Characteristics of the runoff water samples taken in the two rainfall events studied

Sample code	Bottle nº	Total suspension solids (mg L^{-1})		Turbidity (UNF)		Conductivity (µS cm^{-1})	
		Value	Range	Value	Range	Value	Range
1A	4	15	15-16	10.5	10.5-11	55	52-70
1B	11	15		13.5	13.5-13.5	118	118-130
1C	18	16		19	18.6-19	177	176-179
2A	3	8	8-15	4.5	3.5-19	802	98-806
2B	11	12		12		294	
2C	20	15		17		109	

Quantification of MPs in motorway water run-off samples by Py-GC-MS

To quantify microplastics (MPs) in motorway water runoff, glass fibre filters (47 mm diameter, 1 µm pore size) were used to collect particulates from selected samples. Three 5 mm filter aliquots were introduced into the pyrolyser and analysed using the previously validated method for road dust samples (Deliverable D.3.3).

Additionally, total suspended solids (TSS) were quantified by weighing, with values ranging from 8 to 15 mg L^{-1} (Table 4).

Table 4: Total suspended solids of the water runoff samples analysed

Sampling date	Sample Code	Total suspended solids (TSS) (g)	V filtered (L)	[TSS], mg/L
30/04/2024	1A	0.011	0.75	15
	1B	0.008	0.50	15
	1C	0.008	0.50	16
13/05/2024	2A	0.004	0.50	8
	2B	0.006	0.50	12
	2C	0.007	0.50	15

The results obtained by Py-GC-MS for MPs in the runoff samples are summarized in Table 5. Pyrolysis successfully quantified all ten targeted polymers in the motorway water runoff samples. Compared to road dust samples, MP concentrations in runoff were approximately five orders of magnitude lower. However, the most prevalent polymers in the water runoff were like those in road dust, with SBR, ABS, and PE being the most abundant—polymers commonly associated with vehicle-related materials. Furthermore, no significant differences in MP concentrations or distribution were observed between the two rainfall events. The ten quantified polymers were detected in all runoff samples, with SBR (22 %), PE (26 %), ABS (17%), and PA (18 %) being the most representative. These results indicate a consistent MP presence across both rainfall events.

Table 5: Concentration of the analysed polymers (µg L^{-1}) present in the runoff samples by Py-GC-MS

	RAINFALL EVENT 1			RAINFALL EVENT 2		
µg L^{-1}	1A	1B	1C	2A	2B	2C
PS	3.38	1.17	0.54	0.33	2.61	2.36
SBR	26.46	9.27	5.27	5.95	16.25	15.12
PET	2.16	0.57	0.30	1.17	0.91	2.20
PMMA	2.86	3.44	1.74	1.82	2.02	3.13
PC	0.16	0.11	0.07	0.03	0.06	0.07
PA 6	0.16	0.23	0.15	0.07	0.04	0.21
PE	26.48	13.67	11.00	6.69	14.25	13.02
PP	5.82	3.00	2.45	2.08	3.72	2.06
ABS	23.02	6.43	3.07	2.16	14.83	17.35
PA 6,6	13.31	5.83	8.19	10.82	7.97	6.87
Total	**103.8**	**43.7**	**32.8**	**31.1**	**62.7**	**62.4**

3.4 Block Platform for urban drainage and runoff studies

In addition to field studies, tests are carried out on the full-scale urban drainage physical model available at UDC (Figure 29) to study rainfall runoff and pollutant transport, including MP, on surfaces and within the drainage network.

Figure 29: Block Platform for urban drainage and runoff studies at the UDC facilities

For this test, a synthetic road dust sample was used, based on RDS samples taken in the urban tunnel of Avenida Salgado Torres, A Coruña. These samples had been characterised, and the results were presented in Deliverable D3.3. The test was named T1-80mm/H-200g/m^2. Samples were analysed at three selected time points, highlighted in the graph in Figure 30, corresponding to periods with high TSS. The volume of filtered samples, along with TSS, turbidity and conductivity data, is summarised in

Table 6. The samples were filtered using 47 mm diameter glass fibre filters with a 1 µm pore size. In addition, three blank controls were analysed: a filter blank, a blank from the filtration of 500 mL of Milli-Q water, and a field blank consisting of 500 mL of the supply water used in the test. Filters were dried at 40 °C to constant weight after filtration.

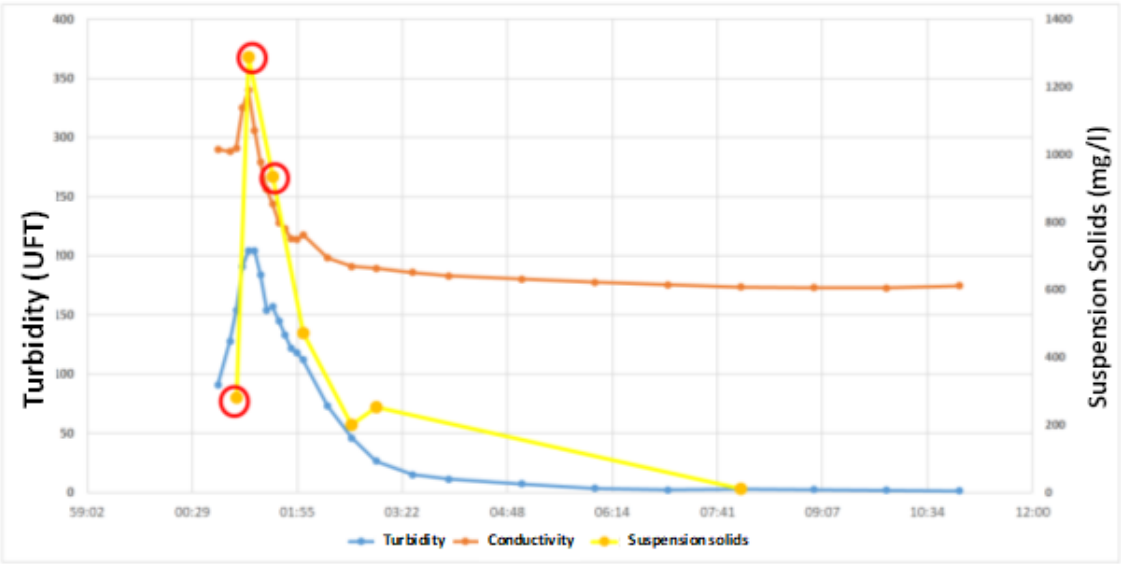

Figure 30: Graph showing selected samples from the Block test and their turbidity, conductivity, and suspended solids measurements.

Table 6: Characteristics of the Block test samples.

Sample code	Bottle nº	V filtrado (mL)	Total suspension solids (mg L^{-1})	Turbidity (UNF)	Conductivity (µs cm^{-1})
T1-80-TW 8A	8	60	283	154	291
T1-80-TW 8B	8	40	250		
T1-80-TW 10A	10	100	960	204	340
T1-80-TW 10B	10	100	1170		
T1-80-TW 14A	14	100	750	157	244
T1-80-TW 14B	14	100	840		

Quantification of MPs in runoff water samples by Py-GC-MS

Microplastics in the runoff water samples from the Block Platform were quantified using Py-GC-MS. The results are presented in Table 7.

Table 7: Concentrations of MPs, expressed as µg L^{-1}, in runoff water samples from the Block Platform

µg L^{-1}	T1-80-TW-8A	T1-80-TW-8B	T1-80-TW-10A	T1-80-TW-10B	T1-80-TW-14A	T1-80-TW-14B
PS	95.1	85.5	129.2	114.4	78.4	53.9
SBR	941.8	664.9	3734	2256	896.8	521.5
PET	116.1	87.8	179.5	99.6	32.4	29.0
PMMA	204.9	232.1	179.5	99.6	32.4	29.0
PC	3.35	2.54	6.55	3.90	2.49	2.68
PA-6	42.1	42.3	72.5	40.5	13.5	9.67
PE	435.1	656.2	667.7	640.4	138.7	144.2
PP	1919	1742	1624	453.1	235.9	203.6
ABS	439.5	400.9	2361	1265	538.6	286.5
PA-6,6	234.5	235.7	273.5	162.5	70.9	55.6
Total	**4432**	**4150**	**9227**	**5135**	**2040**	**1336**

The highest concentration of total polymers (10 MPs quantified) was detected in sample T1-80-TW-10, which coincides with the peak concentration of TSS, as shown in Figure 30. Among the detected polymers, SBR, a key indicator of tyre wear particles, showed the highest concentration, reaching levels three times higher in sample T1-80-TW-10 than in other samples. The dominant polymer was SBR (40 %), followed by ABS (26 %) and PP (18 %), with smaller contributions from PE, PA-6,6, PET, and PMMA.

Additionally, qualitative analysis of the run-off water filters by TD-GC-MS showed the presence of typical tyre marker compounds such as benzothiazole, or 2-(methylthio)benzothiazole, 4-vinylphenol, 4-phenylcyclohexene or 2,2,4-Trimethyl-1,2-dihydroquinoline (TMQ), an antioxidant used as a stabiliser in rubber and tyres. 6PPD, which has been shown to be highly toxic to aquatic organisms (Ihenetu et al., 2024), was also present in these samples. All these compounds have also been found in the qualitative thermodesorption analysis of the above-mentioned motorway road dust samples (see 3.2 for further details).

4 COMPARISON AND EVALUATION OF THE METHODOLOGIES FOR DETECTING MICROPLASTICS IN FIELD SAMPLES

The consortium has implemented different methodologies for detecting MPs across several environmental matrices, including water, sediment, biota, and air from the sample campaigns conducted in the North Sea, Thames River, Elbe River, and Mero-Barcés River Basin.

Based on the acquired experience, the goal of this evaluation is to assess the effectiveness and limitations of each detection technique, considering factors such as the range of measurable particle size or mass determination. In addition, it provides recommendations for best practices in MP extraction and purification, focusing on ensuring polymer preservation and efficient removal of matrix interferences. This evaluation also includes guidelines for quality assurance (QA) and quality control (QC) measures, such as contamination control, blank tests, and ensuring high-quality results.

A variety of spectroscopic and thermal techniques has been used in the analysis of MPs, each with specific size detection limits. Regarding the former, infrared spectroscopy (in any of its measurement modes, transmission, reflection and ATR) dominates most applications. Attenuated Total Reflectance (ATR) FTIR spectroscopy is a widely used option and the usual choice whenever big MPs (500-5000 µm) are to be characterised by means of external accessories. This traditional measurement mode provides fast and accurate measurements for relatively big particles. More advanced approaches involve micro-FTIR (µ-FTIR using an IR microscope). Micro-ATR measurements can be automated or semiautomated depending on the available detector Indeed, micro-ATR with a Germanium or diamond crystal allows measuring particles up to 10 µm, but this involves manual work and it is not a common choice in laboratories. Transmission techniques are currently restricted to the use of FPA (FTIR imaging by focal plane array) detectors allowing measurement for microplastics greater than 10-20 µm. The biggest advantage of FPA-based µ-FTIR is the higher degrees of automation and reduction in analysis time compared with the single-element detector. Other commercial options use linear arrays of 16 detectors with multimode detection (transmission, reflection, ATR imaging). Micro-reflectance IR spectroscopy is a suitable option to avoid the limitations of micro-ATR devices and can measure reliable particles whose size is higher than 30-40 µm (if many spectra are accumulated to improve the signal-to-noise ratio) with an MCT single detector. State-of-the-art chemical imaging methods include transflectance IR spectroscopy based on the use of quantum-cascade lasers (in short, LDIR as it is usually known due to a commercial instrument widely used) which can characterize MPs down to 10 µm, although in manual operation it is possible to reach 5-6 µm using a one-particle-at-a-time approach and using ATR. However, manual operation is not an option when as high amounts as 20,000 particles have to be measured in a single filter. Usually, 20 µm is the current practical limit for transflectance measurements done automatically.

Raman spectroscopy can characterise MPs as small as 1 µm, with micro-Raman achieving even finer resolutions. Automated image processing software has been developed to address these challenges, streamlining analysis time and reducing costs. Hyperspectral Imaging (HSI) is another powerful technique used for larger MPs (> 200-300 µm). It produces a 3D hyperspectral image that integrates spatial and spectral data to provide chemical and morphological insights. However, its main drawback is the complexity of data processing and the need to fix very accurately the illumination of the specimens.

Thermal analysis is increasingly being used to characterise overall quantities of MPs. Techniques such as thermodesorption and pyrolysis coupled with gas chromatography and mass spectrometry detection (TD-GC-MS, Py-GC-MS) provide chemical compositional data and mass-based quantification. However, they do not provide information on particle size, shape or number of particles, and are destructive techniques. Py-GC-MS

is particularly advantageous as it allows the simultaneous identification of polymers and organic additives with minimal sample preparation.

Each technique used in LABPLAS has unique strengths and limitations, so a combined approach is required for comprehensive MP analysis.

4.1 Microplastic mass estimation

Deliverable D6.5 ("Environmental Risk Assessment (E.R.A.) of Plastics in Aquatic and Terrestrial Environments," (submission date: 29/11/2024) presented mass estimations for total MPs associated with river water columns. Two distinct approaches were employed: estimates provided by the simple software (https://simple-plastics.eu/, applied between 10-1000 µm) and those derived from studies conducted by GEOMAR, which considered actual measurements of mass versus area in plastic particles, with a minimum dimension of 0.4 mm.

However, an important question remained unresolved: whether literature-based mass estimations (including those from siMPle) could be considered reliable, especially considering that some of these models had not been extensively tested for smaller particles, such as those found in river water columns (down to 10 µm).

This remains a particularly challenging issue, as standards for small particle mass estimation are not yet available. To address this, additional studies were carried out at UDC.

Several approaches for estimating the mass of MPs in samples have been proposed in the literature. UDC adapted some of these methods (compiled in Barchiesi et al., 2023)) and conducted a comparative study using eleven sets of particles (nine different MP types and two mixtures), whose mass were measured beforehand using a Sartorius ME215P analytical balance (sensitivity: 0.01 mg). The particle sizes ranged from 20 µm and 1500 µm.

The results derived from the six models studied were very unsatisfactory because all of them overestimated the mass. This can be seen in Figure 31, where the most extreme case shows an overestimation of up to (average relative error of 259 %). The models proposed by Isobe et al., 2019 and Medina Faull et al., 2021 exhibited the highest errors.

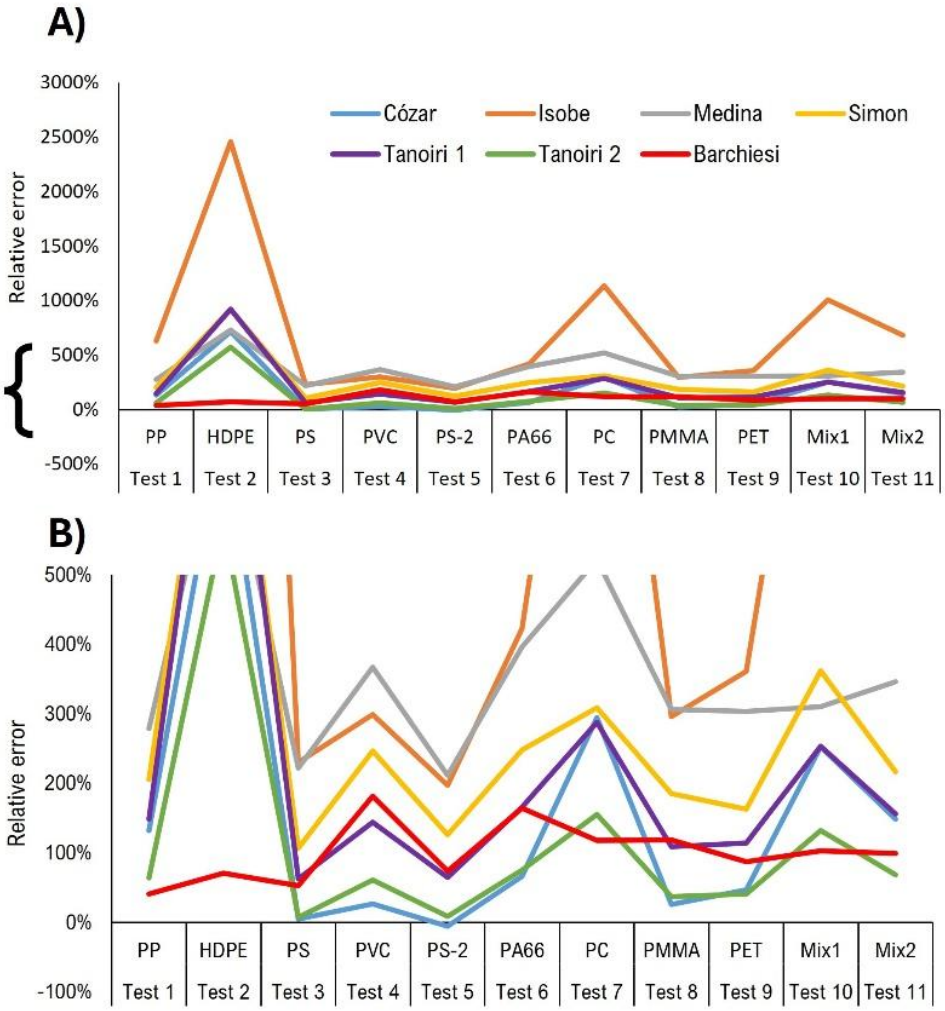

Figure 31: Visualization of the relative errors obtained for A) the eleven particle sets and B) a zoomed view (0 to 500 % error range).

This outcome was somewhat expected, as some models had not been tested for the LDIR imaging system or for small particle sizes, as noted by the original authors (Barchiesi et al., 2023). Here the best-performing model was the one proposed by Barchiesi et al with an average relative error of 107 % and an average RSD of 39 %.

In response to these limitations, UDC adjusted the published models and developed a "hybrid" model, combining equations from different models. These modifications led to significant improvements when applied to the known particle sets. This is particularly important because small particles (< 300 µm) dominate most of the field samples analysed in this project. As a matter of example, Figure 32 illustrates the improvements achieved using the modified models. The overall error was greatly reduced, with maximum errors now around 300 %, and most errors ranging between 50-100 %.

In this case, the best-performing models, based on adaptations from Cózar et al., 2014 (average relative error: 25 %; average RSD: 35 %) and Tanoiri et al., 2021 (average relative error: 17 %; average RSD: 22 %), yielded the most accurate results.

A comprehensive analysis and interpretation of these results will be presented in a scientific manuscript that is under preparation for publication in a peer-review scientific journal.

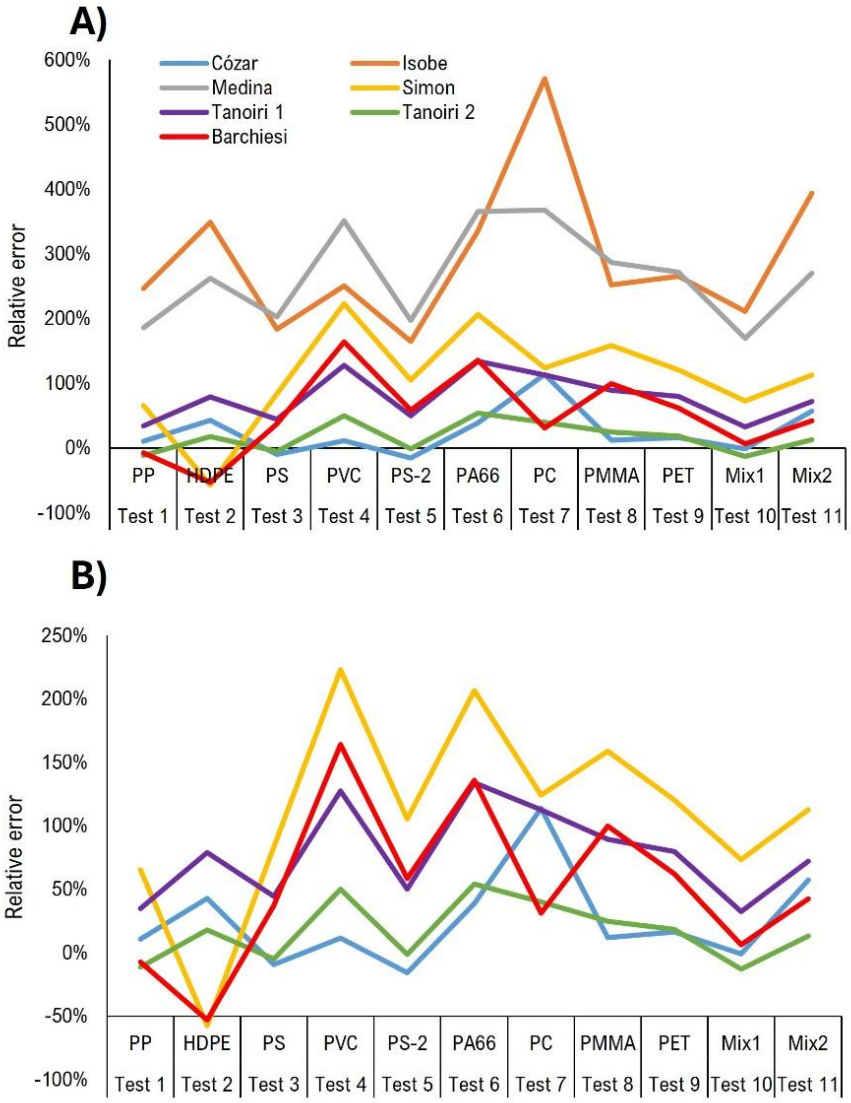

Figure 32: Visualization of the relative errors obtained for the eleven particle sets using A) the modified models and B) the best-performing model.

4.2 Guidelines for quality assurance (QA) and quality control (QC) for MP analysis

Ensuring quality assurance (QA) and quality control (QC) in MP analysis requires strict measures to prevent contamination, degradation, and inaccuracies. Key aspects include sample collection and preparation, contamination control, and analytical method validation.

Sample preparation:

- Biota samples should be collected and stored under conditions that minimize degradation and contamination. Freezing at -20 °C immediately after collection is highly recommended. Formalin is not recommended for MP analysis as it requires extensive washing to remove residual preservative agents and can negatively impact tissue integrity (Ilechukwu et al., 2023).
- Samples must also be protected from direct sunlight and/or strongly bright light.

Contamination control measures:

- Procedural blanks should be conducted alongside the samples and regularly monitored to ensure the absence of MPs within the target size range. Sample results should be reported with blank subtraction, accounting for the corresponding size fraction, polymer type and morphology.
- The overall procedural blanks should embrace control contamination of the laboratory air, field sampling, reagents and transport.
- Ultrapure or microplastics-free water (MPF-water) should be used to prepare all solutions and washing processes and regularly checked to confirm the absence of MPs. Filtration of all reagents and water (0.45 µm) before use is recommended.

Glassware & Equipment:

- All glassware material should be washed with a 17 % HCl solution for 24 h and rinsed with a 1:1 mixture of 96 % ethanol and water before using it. Calcinate metallic filters ≥ 450 °C for at least 3 h. Whenever HCl washing was unsuitable (e.g. for metallic materials), a mixture of 50 % ethanol and 2 % SDS, and ultrasonication for 10-15 min is advisable.
- Avoid using plastic items whenever possible. Whenever possible, replace all plastic materials with glass or metal ones.
- Cover all glassware and unused working items with clean glass Petri dishes or new aluminium foil, and store them upside down to prevent contamination.
- Conduct all sample processing in a laminar flow cabinet, or at the very least sample manipulation and filtration steps and keep the dedicated workspace as clean as possible (it is a good practice to clean the workbench and surroundings with a 1:1 ethanol: water mixture).

Preventive measures for operator contamination:

- Use cotton lab coats with sleeves and particle-free nitrile gloves whenever possible (in many literature reports, gloves are discouraged), and avoid synthetic fibre clothes underneath as far as possible to minimise airborne particle contamination. If synthetic garments are worn, it is good practice to register its/their colour and date, to trace potential operator contamination.

Analytical QA/QC measures:

- Ensure method reliability by using an adequate number of replicates.
- Determine recovery rates and analyse blank controls alongside sample series.
- Consider analytical uncertainties and confidence levels when interpreting results.
- Spectral identification should be done considering reference spectral libraries containing virgin and environmentally aged materials. Other substances than synthetic polymers should be present in the libraries. It is also good practice to include spectra from different particle sizes. Matches must undergo critical evaluation, with visual inspection as a benchmark key validation step. Given the complexity of LDIR spectra, strict HQI thresholds (> 0.90) are recommended for reliable polymer identification. For LDIR spectral analysis, polymer identifications (including particles in the blanks) in the UDC were accepted only if the HQI was > 0.90, or within the 0.85–0.90 range after visual confirmation (López-Rosales et al, 2025b). Rubber identifications were accepted only when HQI > 0.95, following previously established protocols (López-Rosales et al., 2024; Román-Zas et al., 2025). LDIR particle analysis

covered sizes > 20 µm, using a tiered decision criterion to automatically differentiate fibres from fragments (López-Rosales et al., 2024, 2025b). Furthermore, in samples with a large number of particles (> 18,000) a validated sample-based subsampling approach can be considered to streamline the laboratory sample-measurement workload (López-Rosales 2025a).

- Further, whenever ATR and reflectance measurements are made, proper spectral treatments should be applied before comparison with spectral libraries. For example, ATR depth penetration and Kubelka-Munk or Kramers-Kronig treatments for reflectance. Those spectral treatments should be clearly stated in the final reports; as any other spectral treatment.

4.3 Recommendations for best practices in MP sample preparation

In the experience of the LABPLAS project, environmental samples can be categorized into five classes:

- Biota: including bivalves, fish stomachs, and other soft tissues from marine or terrestrial organisms.
- Aqueous samples with organic matter, including plankton, fresh water (from rivers, reservoirs, lakes, etc.), wastewater effluent, and atmospheric deposition.
- Algae: encompasses all types of marine and freshwater plant material.
- Sandy sediments: mainly, beach sands and coarse river sediments.
- Fine sediments: from estuaries, seabed, and soils, with varying levels of organic matter.

Here, general recommendations for the extraction and "purification" of MPs from their matrices are given, with the main emphasis on preserving polymer integrity. Other approaches may be faster, but they should prove they are harmless for MPs. Further, our strategies were developed considering that the final measurements would be FTIR (usually ATR, micro-ATR and/or micro reflectance using a single-point detector) and/or transflectance LDIR analysis. Likely, our recommendations are also good for other particle-based measurement techniques (e.g., FTIR-FPA, Raman or µ-Raman) but some adaptations and refinements might well be required.

For biota samples, enzymatic digestion is the preferred method, as it effectively preserves the integrity of the polymers (López-Rosales et al., 2022). When enzymatic digestion is not feasible due to time constraints, an alkaline digestion method may be a suitable alternative (López-Rosales et al., 2022, 2024). However, macroalgae require a different approach due to their more complex composition (due to, essentially, the carrageenan they contain), necessitating the use of specific enzymes such as cellulase for the effective breakdown of the cellular walls (López-Rosales et al., 2022b).

For aqueous samples (containing different amounts of suspended organic matter), an initial step involving filtration through a metallic stainless-steel filter (10 µm mesh size) is recommended to separate the solid and liquid phases before further processing the former. Once the solid fraction is recovered, the preferred treatment is surfactant-oxidant digestion, which may include the use of Fe^{2+} (Fenton's reagent) when necessary (López-Rosales et al., 2022b). Alternatively, an alkaline-oxidant digestion using NaClO has proved to be an effective approach (López-Rosales et al., 2024).

Sandy sediment samples are usually successfully processed using a differential density separation approach. Out of the many available floating solutions; e.g., sodium polytungstate, NaI, $ZnCl_2$, NaCl, and $CaCl_2$ are commonly used. Considering the most common polymers found in most environmental samples, the cost and toxicity of the reagents, we suggest using $CaCl_2$ and and potassium formate (not still too common but very promising). In contrast, fine-sediment samples require a more thorough treatment. A small amount of sample

is recommended to be taken for further processing to reduce subsequent matrix effects. However, this may affect the overall sample representativity and it may require analysing multiple aliquots to reliably characterise the sample (or the site). Initial sieving can be an alternative approach to avoid matrix effects (mostly, the flotation of fine particles due to the matrix), but this poses the risk of losing MPs smaller than 63 µm, thereby limiting the detection capabilities. For complex matrices containing both organic and inorganic matter, such as sewage sludge, a tailored strategy is required. Depending on the sample composition, density separation may need to be performed before digestion, or vice versa. If the sample is organic matter-rich (e.g., secondary sludge), digestion should be prioritised, whereas for inorganic-rich (e.g., primary sludge), density separation is the recommended first step. Properly selecting the initial processing step is crucial, as it helps avoid unnecessary complications and reduces the overall processing time (Elkhatib and Oyanedel-Craver, 2020) (van den Berg et al., 2020).

5. REFERENCES

Barchiesi, M., Kooi, M., Koelmans, A.A., 2023. Adding Depth to Microplastics. Environ. Sci. Technol. 57, 14015–14023. https://doi.org/10.1021/acs.est.3c03620.

Cózar, A., Echevarría, F., González-Gordillo, J.I., Irigoien, X., Úbeda, B., Hernández-León, S., Palma, Á.T., Navarro, S., García-de-Lomas, J., Ruiz, A., Fernández-de-Puelles, M.L., Duarte, C.M., 2014. Plastic debris in the open ocean. Proc. Natl. https://doi.org/10.1073/pnas.1314705111

Elkhatib, D., Oyanedel-Craver, V. A Critical Review of Extraction and Identification Methods of Microplastics in Wastewater and Drinking Water. Environmental Science & Technology, 2020, 54(12), 7037−7049. Doi/10.1021/acs.est.9b06672.

Enders K, Lenz R, Ivar Do, Sul JA, et al., 2020. When every particle matters: A QuEChERS approach to extract microplastics from environmental samples. MethodsX 7: 100784.

Hildebrandt, L., Gareb, F.E, Zimmermann, T., Klein, O., Kerstan, A., Emeis, K.C., Pröfrock, D., 2020. Agilent Application Note: Fast, Automated Microplastics Analysis Using Laser Direct Chemical Imaging - Characterizing and Quantifying Microplastics in Water Samples from Marine Environments.

Hildebrandt, L., Gareb, F.E, Zimmermann, T., Klein, O., Kerstan, A., Emeis, K.C., Pröfrock, D., 2022. Spatial distribution of microplastics in the tropical Indian Ocean based on laser direct infrared imaging and microwave-assisted matrix digestion. Environmental Pollution 307, 119547.

Ilechukwu, I., Das, R.R., Reimer, J.D., 2023. Review of microplastics in museum specimens: An under-utilized tool to better understand the Plasticene, Marine Pollution Bulletin, 191, 114922. https://doi.org/10.1016/j.marpolbul.2023.114922.

Ihenetu, S.C., Xu, Q., Khan, Z.H., Kazmi, S.S, Ding, J., Sun, Q., Li, G., 2024. Environmental fate of tire-rubber related pollutants 6PPD and 6PPD-Q: A review. Environmental Research, 258, 119492. https://doi.org/10.1016/j.envres.2024.119492.

Isobe, A., Iwasaki, S., Uchida, K., Tokai, T., 2019. Abundance of non-conservative microplastics in the upper ocean from 1957 to 2066. Nat. Commun. 10, 417. https://doi.org/10.1038/s41467-019-08316-9.

Kaiser, J., Abel, S., Arz, H. W., Cundy, A. B., Dellwig, O., Gaca, P., Gerdts, G., Hajdas, I., Labrenz, M., Milton, J. A., Moros, M., Primpke, S., Roberts, S. L., Rose, N. L., Turner, S. D., Voss, M., & Ivar do Sul, J. A., 2023. The

East Gotland Basin (Baltic Sea) as a candidate Global boundary Stratotype Section and Point for the Anthropocene series. The Anthropocene Review, 10(1), 25-48.

López-Rosales, A., Andrade, J., Fernández-González, V., López-Mahía, P., Muniategui-Lorenzo, S., 2022a. A reliable method for the isolation and characterization of microplastics in fish gastrointestinal tracts using an infrared tunable quantum cascade laser system. Marine Pollution Bulletin 178, 113591. https://doi.org/10.1016/j.marpolbul.2022.113591. Open Access.

López-Rosales A, Andrade JM, López-Mahía P, Muniategui-Lorenzo S. 2022b Development of an analytical procedure to analyze microplastics in edible macroalgae using an enzymatic-oxidative digestion. Marine Pollution Bulletin 2022;183:114061. https://doi.org/10.1016/j.

López-Rosales, A., Ferreiro, B., Andrade, J., Fernández-Amado, M., González-Pleiter, M., López-Mahía, P., Rosal, R., Muniategui-Lorenzo, S., 2024. A reliable method to determine airbone microplastics using quantum cascade laser infreared spectrometry. Science of The Total Environment, 913, 169678. https://doi.org/10.1016/j.scitotenv.2023.169678. Open Access.

López-Rosales, A., Andrade, J., Ferreiro, B., Muniategui-Lorenzo, S., 2025a. Sample-based subsampling strategies to identify microplastics in the presence of a high number of particles using quantum-cascade laser-based infrared imaging. Talanta, 292, 127915. https://doi.org/10.1016/j.talanta.2025.127915.

López-Rosales A, Ferreiro B, Andrade JM, Kerstan A, Robey D, Muniategui S. 2025b; Reviewing the fundamentals and best practices to characterize microplastics using state–of–the-art quantum-cascade laser reflectance-absorbance spectroscopy. TrAC Trends in Analytical Chemistry 188:118229. https://doi.org/10.1016/j.trac.2025.118229.

Medina Faull, L.E., Zaliznyak, T., Taylor, G.T., 2021. Assessing diversity, abundance, and mass of microplastics (~ 1–300 μm) in aquatic systems. Limnol. Oceanogr. Methods 19, 369–384. https://doi.org/https://doi.org/10.1002/lom3.10430.

Román-Zas, C., Ferreiro, B., Terán-Baamonde, J., Del Castillo Busto, M.E., Andrade, J.M., Muniategui, S., 2025. Measurement of tyre-based microplastics using traditional and quantum cascade laser-based infrared spectrometry. Spectrochim Acta Part A: Molecular and Biomolecular Spectroscopy 2025, 327, 125321. Open Access.

Tanoiri, H., Nakano, H., Arakawa, H., Hattori, R.S., Yokota, M., 2021. Inclusion of shape parameters increases the accuracy of 3D models for microplastics mass quantification. Mar. Pollut. Bull. 171, 112749. https://doi.org/10.1016/j.marpolbul.2021.112749.

Van den Berg, P., Huerta-Lwanga, E., Corradini, F., Geissen, V. Sewage sludge application as a vehicle for microplastics in eastern Spanish agricultural soils. Environmental Pollution, 2020, 261, 114198. oi.org/10.1016/j.envpol.2020.114198.

Wang, Y., Fu, R., Sun, P. *et al*, 2023. Screening eco-friendliness tire antioxidants alternatives: functional 2,2,4-trimethyl-1,2-dihydroquinoline derivatives design and toxicity evaluation. *Environ Sci Pollut Res* 30, 92282–92294. https://doi.org/10.1007/s11356-023-28836-8.

Waters, C., Turner, S., An, Z., Barnosky, A., Cearreta, A., Cundy, A., Fairchild, I., Fiałkiewicz-kozieł, B., Gałuszka, A., Grinevald, J., Hajdas, I., Han, Y., Head, M., Ivar do Sul, J., Jeandel, C., Leinfelder, R., Mccarthy, F., Mcneill,

J., Odada, E., Zinke, J., 2024. Executive Summary: The Anthropocene Epoch and Crawfordian Age: proposals by the Anthropocene Working Group. 10.31223/X5VH70.

Whiting, Q.T., O'Connor, K.F., Potter, P.M., Al-Abed, S.R., 2022. A high-throughput, automated technique for microplastics detection, quantification, and characterization in surface waters using laser direct infrared spectroscopy. Analytical and Bioanalytical Chemistry 414, 8353–8364. https://doi.org/10.1007/s00216-022-04371-2.